Valkyrie Probes: A Novel Class of Enzyme-Activatable Photosensitizers based on Sulfur- and Seleno-Rosamines with Pyridinium Unit

Vivian Lioret, Kévin Renault, Olivier Maury, Anthony Romieu

ACES Asian Chemical Editorial Society

doi.org/10.1002/asia.202300756

CHEMISTRY AN ASIAN JOURNAL Research Article

www.chemasianj.org

Valkyrie Probes: A Novel Class of Enzyme-Activatable Photosensitizers based on Sulfur- and Seleno-Rosamines with Pyridinium Unit**

Vivian Lioret[+],*[a] Kévin Renault[+],*[a, b] Olivier Maury,[c] and Anthony Romieu*[a]

Dedicated to Dr. Jean Cadet for his major contribution to the research field of DNA photosensitization reactions

The rational design of activatable photosensitizers (aPSs) uncaged by specific disease biomarkers is currently booming due to their positive attributes to achieve targeted photodynamic therapy (PDT). In this context, we present here the synthesis and detailed photophysical characterization of a novel class of hetero-rosamine dyes bearing sulfur or selenium as bridging heavy atom and 4-pyridyl *meso*-substituent as optically tunable group. The main feature of such photoactive platforms is the spectacular change of their spectral properties depending on the caging/decaging status of their 4-pyridyl moiety (cationic pyridinium *vs.* neutral pyridine). The preparation of two alkaline phosphatase (ALP)-responsive probes (named Valkyrie probes) was achieved through formal *N*-quaternarization with 4-phosphoryloxybenzyl, the traditional recognition moiety for this important diagnostic enzyme. Bio-analytical validations including fluorescence/singlet oxygen phosphorescence enzyme assays and RP-HPLC-fluorescence/-MS analyses have enabled us to demonstrate the viability and effectiveness of this novel photosensitizer activation strategy. Since sulfur-containing Valkyrie probe also retains high fluorogenicity in the orange-red spectral range, this study highlights *meso*-pyridyl-substituted S-pyronin scaffolds as valuable candidates for the rapid construction of molecular phototheranostic platforms suitable for combined fluorescence diagnosis and PDT.

Introduction

The ability to selectively ablate or destroy abnormal cells or tissues without affecting the surrounding healthy area is a major therapeutic challenge in the fight against numerous diseases, such as cancers.[1] Alongside strategies developed and currently used for cancer treatment like chemotherapy, radiotherapy, surgery, and more recently targeted immunotherapy, photodynamic therapy (PDT) has emerged as a less invasive and generally more selective therapeutic modality.[2] Indeed, this latter one utilizes a low-energy light (*i.e.*, "gentle" visible or near-infrared (NIR) light) to trigger the cascade of events yielding positive treatment outcomes. From molecular point of view, the light absorbing species involved in this process, named photosensitizer (PS), is promoted to higher energy state S_n, then rapidly undergoes internal conversion (IC) and vibrational relaxation to the lowest vibrational level in S_1 (Kasha's rule), and finally reaches the first triplet excited state T_1 by intersystem crossing (ISC) process. The subsequent relaxation pathways regarded as the prominent source of PDT effect, are type I and type II photosensitized oxidation reactions.[3] Type I mechanism can be briefly described as a direct interaction between excited ^{3}PS with molecular substrates (typically, key biomolecules of cancer cells) to form pairs of neutral radicals or radical ions, which then react with surrounding water or oxygen to yield oxidized/oxygenated products, and/or toxic reactive oxygen species (ROS) including superoxide anion ($O_2^{\bullet-}$) and hydroxyl radicals ($^\bullet$OH) also capable of damaging tumor cells components. Conversely, type II mechanism involves a direct energy transfer from ^{3}PS to molecular oxygen, that produces singlet oxygen ($^1O_2$).[4] This non-radical species is a better oxidizing agent than ground state oxygen ($^3O_2$) and identified as a potent and reactive dienophile, that promotes degradation of nucleic acids (exclusively guanine base), unsaturated lipids and some amino

[a] *Dr. V. Lioret,[+] Dr. K. Renault,[+] Prof. Dr. A. Romieu*
Institut de Chimie Moléculaire de l'Université de Bourgogne, UMR 6302, CNRS
Université de Bourgogne
9, Avenue Alain Savary
21000 Dijon (France)
E-mail: vivianlioret.vl@gmail.com
kevin.renault@curie.fr
anthony.romieu@u-bourgogne.fr

[b] *Dr. K. Renault[+]*
Present address:
CNRS UMR9187, Inserm U1196, Chemistry and Modeling for the Biology of Cancer Institut Curie, Université PSL, 91400, Orsay (France)
E-mail: kevin.renault@curie.fr

[c] *Dr. O. Maury*
University of Lyon, Laboratoire de Chimie, UMR 5182, CNRS, ENS Lyon
46, Allée d'Italie
69364 Lyon (France)

[+] *These authors contributed equally to this work.*

[**] *A previous version of this manuscript has been deposited on a preprint server (DOI: 10.26434/chemrxiv-2023-xr1b4-v2).*

Supporting information for this article is available on the WWW under https://doi.org/10.1002/asia.202300756

acids (*i.e.*, tryptophan, histidine and methionine).[5] The simultaneous presence of the three partners (PS, visible or NIR light and molecular oxygen) is very often required to witness a therapeutic effect, giving to this photomedicine technique high selectivity. Indeed, PS photoactive molecule stays in an "OFF" status as long as it is not subjected to irradiation. However, it can be overwhelming to accumulate PS molecules in abnormal tissues while avoiding their scattering in healthy areas, which causes undesired photodamages during the excitation process. Historically, the first generation of PS agents, based on tetrapyrrolic macrocycles such as hematoporphyrin or photofrin, accumulates in cancer cells thanks to the enhanced permeability and retention effect (EPR), thus often inducing non-optimal selectivity towards cancer cells and producing significant off-target phototoxicity and side-effects. This is a major drawback and probably the main current challenge associated with PDT to be overcome, in order to definitely popularize this technique as a suitable therapeutical option in clinical settings. Among the different strategies explored to enhance targeting properties of PS agents,[6] one based on the preparation and administration of photo-immunoconjugates (PICs, *i.e.*, antibodies armed with PS molecules) has received considerable attention during the past decade.[7] This approach named photo-immunotherapy (PIT), takes advantage of unsurpassed ability of antibodies to recognize and bind tumor-associated antigens, and thus delivering PS molecules selectively to the cancer cells. However, the main limitation to this targeted PDT is closely linked with the degree of labeling (DOL, *i.e.*, number of PS molecules covalently linked per antibody) of PICs that must be low to maintain targeting properties of parent antibody.[8] As this biological vector is hundreds of times larger than the PS molecule, a limited amount of photoactive compound is thus administrated and suboptimal PDT effect may be obtained. An alternative and/or complementary strategy to PIT involves the use of analyte-responsive PS agents rationally designed using protection-deprotection strategies historically implemented in reaction-based fluorogenic probes[9] (*i.e.*, fluorescent chemodosimeters[10]). Indeed, the masking of a key functional group found in the chromophore structure induces marked changes in electronic properties and makes PS in an "OFF" state (inactivated PS). Conversely, analyte-triggered deprotection of this optically tunable group promotes PS in an "ON" status (activated PS), resulting in the recovery of its photoactivity. Such activatable photosensitizers (aPSs)[6a,11] are particularly well suited for targeted PDT[12] because of their ability to selectively respond to a biological stimulus such as a reactive biomarker specifically overexpressed in disease cells and tissues (*e.g.*, enzymes, biothiols, ROS, …).[13] Consequently, targeted activation allows aPS capable of distinguishing healthy cells from diseased ones, thus minimizing off-target phototoxicity during PDT. Since some PS agents also maintain acceptable fluorescence properties, the fluorogenic behavior of their activatable counterparts might also be exploited for real-time monitoring of the analyte-triggered PS activation and thus enabling imaging-guided PDT.[14] In the quest for high-performance aPS agents that may combine optimal photosensitization properties and possibly a good fluorogenic behavior in response to a specific enzyme activity, associated with ease of synthesis, we have recently revisited the chemistry of hetero-rosamine dyes highlighted in the early 2000s by the Detty group (Figure 1).[15] Indeed, the replacement of intracyclic oxygen atom by a heavy heteroatom (sulfur,[15a,16] selenium[15a,16–17] and more recently bismuth-phenyl moiety[18]) has been identified as an effective way to convert fluorescent tetramethylrosamine dyes into red-light excitable photosensitizers through promoting ISC process. The facile conversion of Se-rosamine/rosol dyes into the corresponding enzyme-responsive aPS agents was considered later in 2014–2019 and jointly achieved by the groups of Hanaoka and Urano (Figure 1).[19,20] Molecular desymmetrization of hetero-xanthene scaffold through incorporation of a primary aniline or phenol moiety enables the facile installation of enzymatic recognition moiety (*i.e.*, 4-(dimethylamino)phenylazo moiety for azoreductase (AzoR), β-galactosyl moiety for β-galactosidase (β-Gal) and γ-glutamyl moiety for γ-glutamyltranspeptidase (γGT)) required for "OFF-ON" switching mechanism. However, the synthesis of such unsymmetrical Se-xanthene dyes is not a trivial task, and the modulation of their photophysical properties is only achieved through the conventional protection-deprotection strategy of amino or hydroxyl group, and intramolecular spirocyclization reaction when *meso*-phenyl is *ortho*-substituted with an hydroxymethyl group. This latter also makes their synthetic accessibility difficult and impedes facile exemplification of the "center atom substitution" strategy applied to xanthene-based aPSs, to a wide range of biological stimuli through the implementation of different activation mechanisms. To circumvent such limitations, the contribution from the Ge group in the field of rosamine-based fluorescent probes may be of valuable help.[21] Indeed, they identified the 4-pyridyl unit installed at the *meso* position as an effective fluorogenic reactive center for xanthene scaffold through an *N*-alkylation-dealkylation process. The low fluorescence of the corresponding pyronin-pyridinium hybrid structure was explained in terms of oxidative photo-induced electron transfer (d-PeT) process from the excited state of fluorescent pyronin group to the *N*-alkylpyridinium substituent LUMO (Figure 1).[22] Analyte-triggered self-immolative *N*-dealkylation process leads to the release of strongly fluorescent rosamine with pyridine unit, the effects of d-PeT being prohibited. Several biomarkers including enzymes (nitroreductase, NTR),[21c] gasotransmitters (hydrogen sulfide, H_2S)[21a,b] and ROS (hydrogen peroxide, H_2O_2)[21b] have been successfully detected in solution and in cellular imaging, using this reaction-based approach. Furthermore, the use of a symmetrical rosamine dye as fluorescent reporter facilitates access to these probes. Interestingly, this fluorogenic probe design principle was recently extended to a longer wavelength silicon analog (pyridine-Si-rosamine) for imaging cysteine and ROS both in cells and *in vivo*.[23] Inspired by these works, we propose here new symmetrical sulfo- and seleno-rosamines dyes (S- and Se-rosamine dyes) bearing the optically tunable 4-pyridyl group as *meso*-aryl substituent, and synthetized using an original way (Figure 1). *N*-quaternization for incorpo-

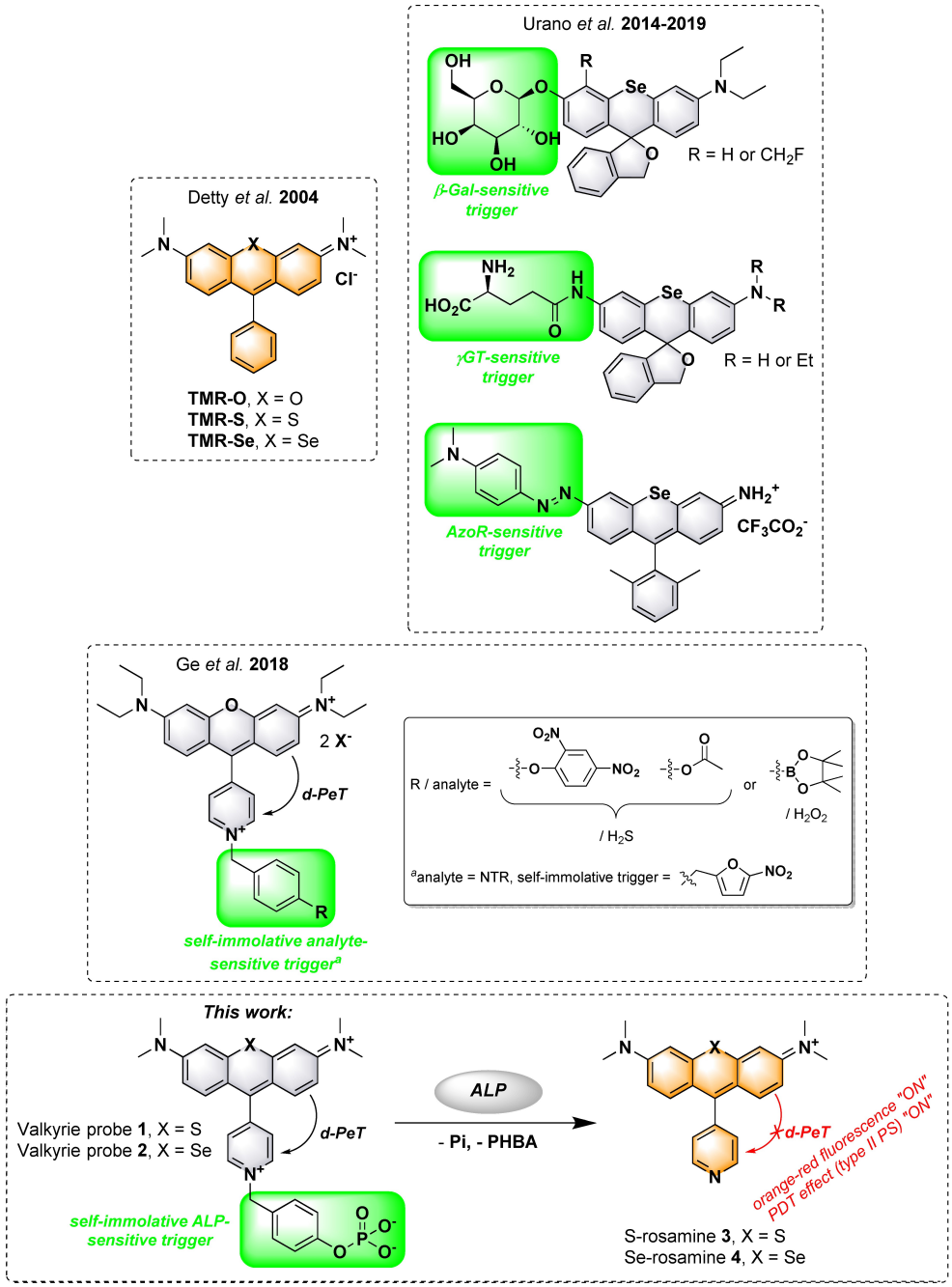

Figure 1. (Top) Current state of the art of (enzyme-activatable) type II photosensitizers based on **TMR-O** (left) or related hetero-rosamine/rosol scaffolds (right); (middle) analyte-responsive fluorescent probes based on a pyronin-pyridinium hybrid structure, developed by the Ge group; (bottom) enzyme-activatable type II photosensitizers expored in this work, based on hetero-rosamine scaffolds and pyridine caging/decaging strategy. [ALP = alkaline phosphatase, AzoR = azoreductase, β-Gal = β-galactosidase, γGT = γ-glutamyltranspeptidase, NTR = nitroreductase, PDT = photodynamic therapy, d-PeT = oxidative photo-induced electron transfer, PHBA = *para*-hydroxybenzyl alcohol, Pi = phosphate anion, PS = photosensitizer, **TMR-O** = tetramethylrosamine, **TMR-S** = tetramethyl-S-rosamine, **TMR-Se** = tetramethyl-Se-rosamine, X^- = counter ion not specified]. Please note: the color of the structure indicates approximately the spectral range of its emission: grey = non-fluorescent, orange = fluorescence emission of **TMR-S** or S-rosamine **3**. To avoid overloading figure, yellow emission of **TMR-O** is not shown; **TMR-Se** and Se-rosamine **4** are not or poorly fluorescent.

rating a specific molecular recognition moiety of a given enzyme activity, is being considered to make these hetero-xanthene-based photoactive compounds activatable under the action of alkaline phosphatase (ALP),[24] an important enzyme in living organisms, and frequently used as a relevant biomarker of several human diseases (*e.g.*, blood diseases such as anemia and leukemia, bone diseases, liver dysfunctions and cancers).[25]

Herein, we report the synthesis of these novel hetero-rosamines and the corresponding ALP-responsive pyridinium-based probes which we called Valkyrie probes (the word "Valkyrie" comes from the Old Norse word "valkyrja" meaning a "chooser of the dead"). A comprehensive photophysical study

notably involving the determination of singlet oxygen quantum yields (Φ_Δ) through two distinct comparative methods (*i.e.*, phosphorescence measurements of $^1O_2$ and UV-vis absorbance decay of $^1O_2$ chemical trap 1,3-diphenylisobenzofuran (DPBF)), and *in vitro* enzyme assays were carried out to confirm the assumed spectral "OFF-ON" behavior of such aPSs, upon activation by ALP. For S-rosamine derivative that is also able to produce an intense fluorogenic "OFF-ON" response, the implementation of a robust analytical methodology based on RP-HPLC-fluorescence and RP-HPLC-MS analyses has also been envisaged with the aim of deciphering the ALP-sensing mechanism involved in this novel class of photoactive probes.

Results and Discussion

Synthesis of hetero-rosamine dyes bearing 4-pyridyl unit as *meso*-aryl substituent, and related Valkyrie probes

The synthetic route devised to obtain sulfur and selenium analogs of pyronin-pyridine hybrid structure previously studied by the Ge group,[21] is depicted in Scheme 1. The strategy is based on an acid-mediated condensation between a symmetrical bis-aryl thio- or selenoether and commercial 4-pyridinecarboxaldehyde. Facile *N*-quaternarization of their *meso*-(4-pyridyl) unit with the traditional phosphatase recognition moiety based on a self-immolative spacer (*i.e.*, 4-phosphoryloxybenzyl)[26] enables the conversion of these hetero-rosamine dyes **3** and **4** into the corresponding ALP-responsive S/Se-rosamine-based probes **1** and **2**. First, symmetrical bis-aryl thioether **5** was prepared through a copper-catalyzed C–S cross-coupling reaction between 3-iodo-*N*,*N*-dimethylaniline (1.7 equiv.), readily prepared from 3-iodoaniline by reductive amination,[27] and Na_2S hydrate (6.5–7H_2O) under conditions reported by Deng *et al.* (CuI (0.1 equiv.), K_2CO_3 (1.7 equiv.), degassed DMF, 120 °C, 18 h).[28] This diaryl sulfide was purified by flash-column chromatography over silica gel. The same reaction was also attempted using 3-bromo-*N*,*N*-dimethylaniline because of its commercial availability at a reasonable price. However, this aryl bromide was found to be totally unreactive towards sulfide anion under the conditions described above. In a more original way, the implementation of such Ullmann-type carbon-chalcogen bond-forming reaction with sodium selenide (Na_2Se) was next considered for the first time in order to simplify synthetic route towards bis-aryl selenoethers. Indeed, such compounds are typically prepared through a non-trivial organolithium route that requires both tedious preparation of bis[3-(dialkylamino)phenyl] diselenide and generation of an aryl lithium compound from the corresponding aryl halide to achieve coupling between them,[29] all steps conducted under drastic anhydrous conditions. Reaction of 3-iodo-*N*,*N*-dimethylaniline (1.7 equiv.) with Na_2Se

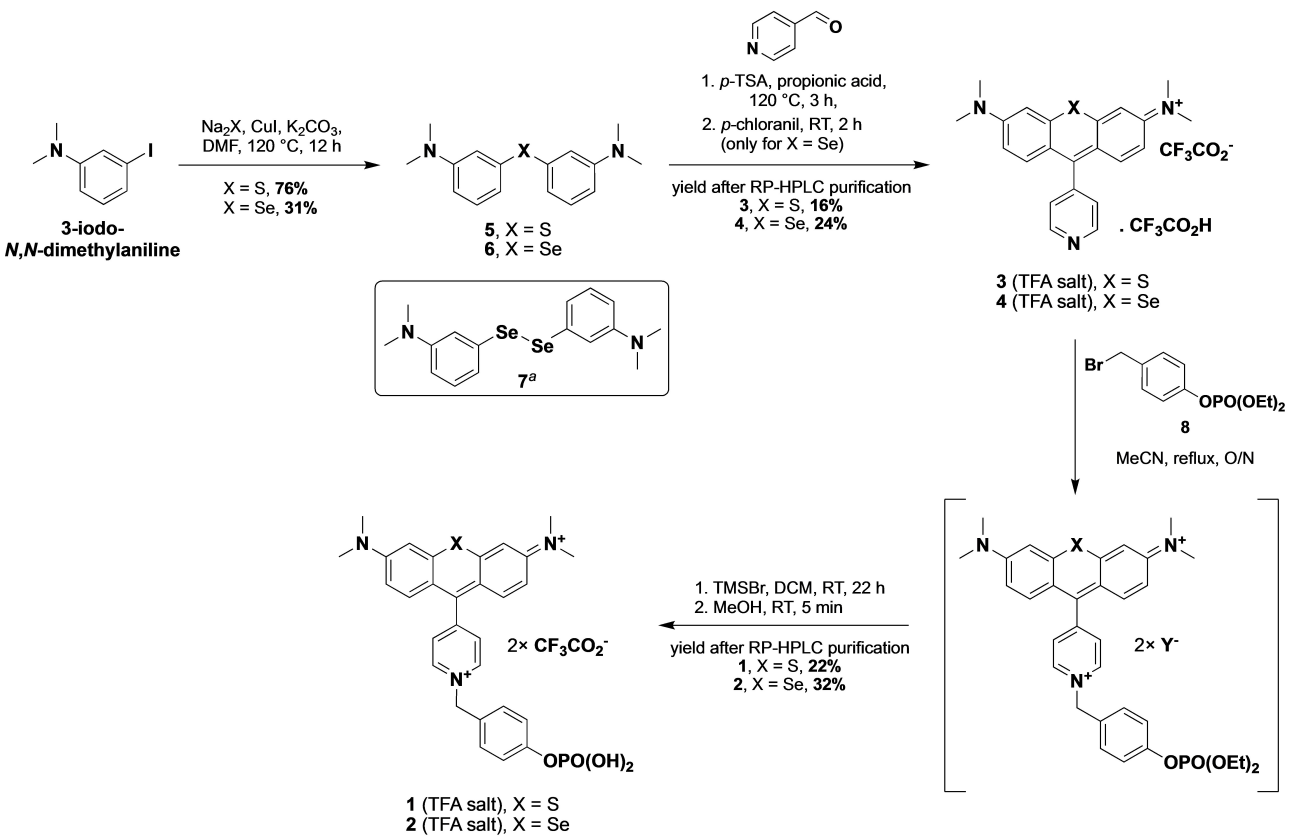

Scheme 1. Synthesis of hetero-rosamine dyes **3** and **4**, and ALP-responsive Valkyrie probes **1** and **2**. [a] Please note: this compound named 3,3′-diselenobis[*N*,*N*-dimethylbenzenamine], is the major product of the Ullmann-type C–Se cross-coupling reaction. [O/N = overnight, RT = room temperature, TMSBr = trimethylsilyl bromide, *p*-TSA = *para*-toluenesulfonic acid, $Y^- = Br^-$ or $CF_3CO_2^-$].

(two successive additions of 1.0 equiv., separated by 12 h) in the presence of CuI (0.17 equiv.) and K_2CO_3 (1.7 equiv.), in dry DMF, at 120 °C, led to the desired symmetrical bis-aryl selenoether **6** mixed with the diaryl diselenide derivative **7** and a minor amount of starting aryl iodide (see Supporting Information for the RP-HPLC-MS analysis of the crude reaction mixture, Figure S23). Isolation of **6** in a pure form was achieved by flash-column chromatography over silica gel, with a moderate 31% yield. Thereafter, bis[3-(dimethylamino)phenyl] sulfide and selenide **5** and **6** were reacted with 4-pyridinecarboxaldehyde under acidic conditions (propionic acid as solvent and *para*-toluenesulfonic acid (*p*-TSA) as catalyst) and heated in a sealed tube at 120 °C. For the formation of S-rosamine dye **3**, a reaction time of 3 h was found to be the best compromise between a satisfying conversion rate and the limited formation of undesired side-products. In the case of the selenium analog, the same conditions provided a 1:1 mixture of Se-rosamine **4** and its reduced form. Complete aromatization of this latter compound was achieved by a further treatment with *para*-chloranil (1 equiv.) at room temperature for 2 h. After work-up (neutralization) of crude acidic mixtures, the two hetero-rosamines were directly purified by semi-preparative RP-HPLC and recovered as TFA salts after freeze-drying (isolated yield: 16% for **3** and 24% for **4** based on TFA mass = 48.2% (2.9 molecules) and 42.9% (2.7 molecules) respectively). All spectroscopic data, especially NMR and ESI mass spectrometry, were in agreement with the structures assigned for both hetero-pyronin-pyridine hybrid structures. Final conversion into Valkyrie probes **1** and **2**, by incorporating the ALP recognition moiety into *meso*-(4-pyridyl) unit was achieved by *N*-alkylation with diethyl 4-(bromomethyl)-phenylphosphonate **8** in refluxing MeCN. After complete conversion into the corresponding *N*-alkylpyridinium salts (confirmed by RP-HPLC-MS analyses), the reaction mixtures were concentrated under reduced pressure and the crude products were directly subjected to a prolonged treatment (22 h) with an excess of TMSBr (5 equiv.) in dry DCM at room temperature, to perform complete deprotection of phosphate moiety. Purification by semi-preparative RP-HPLC provided TFA salts of ALP-responsive S/Se-rosamine-based probes with satisfying isolated yields (22% for **1** and 32% for **2**, over two steps, and based on TFA mass = 28.9% (1.9 molecules) and 32.8% (2.5 molecules)) and optimal purity (> 97%) suitable for photophysical measurements and *in vitro* enzyme assays. Their structures were unambiguously confirmed by ESI-LRMS and NMR (^{1}H, ^{13}C, ^{19}F and also ^{77}Se for **2**) spectroscopic analyses (see Supporting Information).

Photophysical properties of hetero-rosamine dyes and ALP-responsive Valkyrie probes

For the determination of absorption and fluorescence features of these novel xanthene derivatives, we have selected two distinct aqueous buffers (phosphate buffered saline (PBS, 10 mM phosphate + 2.7 mM KCl and 137 mM NaCl), pH 7.3 as simulated physiological conditions, and Tris.HCl buffer pH 8.0 well suited for *in vitro* enzyme assays with ALP[25,30]), and DMSO. The permanent mono- or dicationic charge makes those dyes and probes a remarkable solubility in water and in polar solvents, especially under neutral pH conditions. The specific photophysical properties are compiled in Table 1 and the corresponding electronic absorption, excitation, and emission spectra are available in Figure 2 (illustrative examples of spectra obtained in PBS with S- and Se-rosamines **3** and **4**) and in the Supporting Information. Whatever the solvent used, the shape of the absorption spectrum of each compound is typical of the spectral signature observed for some heteroatom-substituted analogs of xanthene dyes: (1) an intense absorption band with a maximum in the range 580–600 nm, assigned to the 0–0 band of the S_0-S_1 transition, and (2) a shoulder peak on the high-energy side (around 550–560 nm) corresponding to vibronic pattern. By replacing the sulfur-bridge atom by selenium, a further but modest bathochromic shift of 10 nm was obtained. As demonstrated in numerous published studies, in particular, contributions from the Detty and Dieng groups,[15a,28] the remarkable red-shift of absorption curves compared to those of traditional rosamine/rhodamine dyes bearing the lighter chalcogen (oxygen) as the bridging atom, is rationalized through the sole reduction in LUMO energy. Indeed, a higher contribution of S/Se atom in the π*-system *via* enhanced p*-π* conjugation, leads to this lowering effect. Interestingly, *N*-quaternarization of *meso*-(4-pyridyl) unit with ALP-responsive unit strengthens the push-pull character of Valkyrie probes **1** and **2** for which intramolecular charge transfer is exalted leading to more red-shifted absorption (ca., 15–20 nm depending on the solvent used). The fluorescence properties of S- and Se-rosamines **3** and **4** within the orange-red spectral range, are also in line with some published results. A moderate emission whose maximum ranges between 608 nm (PBS) and 621 nm (DMSO) was observed for sulfur-modified xanthene dye **3**. Values of relative fluorescence quantum yields do not exceed 20%, which is indicative of the increasing prominence of ISC process to T_1 excited state, promoted by heavy-atom effect. The formation of non-emissive aggregates (*i.e.*, H-type homodimers) known to also negatively impact brightness, was ruled out because a perfect matching between the absorption and excitation profiles was observed in aqueous buffers (PBS or Tris.HCl) for concentrations within the range 5–15 μM. Even if we managed to detect residual fluorescence emission of selenium analog **4** centered at 613 nm (PBS) or 626 nm (DMSO), relative fluorescence quantum yield values lower or equal to 1% were determined, underlining the greater ability of this heavier chalcogen atom to promote triplet formation relative to fluorescence.

By analogy with the pyronin-pyridine hybrid structure extensively studied by the Ge group,[15a,28] *N*-quaternarization of *meso*-(4-pyridyl) unit of **3** and **4** with enzymatic recognition moiety, was found to be an effective way to quench their moderate/low orange-red fluorescence through modulation of d-PeT mechanism. In the case of Valkyrie probe **3**, the formation of an electron-withdrawing pyridinium moiety through *N*-alkylation resulted in the disappearance of typical fluorescence signature of xanthene dyes and the occurrence of a strongly Stokes-shifted ICT emission band centered at ca. 680 nm and

Table 1. Photophysical properties of hetero-rosamine dyes and ALP-responsive Valkyrie probes at 25 °C.

Cmpd[a]	Solvent	Abs max[b] [nm]	Em max [nm]	Stokes shift [cm^{-1}]	ε [M^{-1} cm^{-1}]	Φ_F[c] [%]
3	DMSO	591	621	817	98050	19
	PBS (pH 7.3)	580	608	794	86750	14
	Tris.HCl buffer (pH 8.0)	580	605	712	89950	14
4	DMSO	601	626	664	114000	–[d]
	PBS (pH 7.3)	591	613	607	101600	–[d]
	Tris.HCl buffer (pH 8.0)	590	613	636	112500	–[d]
VLKR probe **1**	DMSO	602	677	1840	77050	4
	PBS (pH 7.3)	595	678	2057	81750	1
	Tris.HCl buffer (pH 8.0)[]	594	678	2085	78850	1
VLKR probe **2**	DMSO	611	–[d]	–[d]	79500	–[d]
	PBS (pH 7.3)	604	–[d]	–[d]	96300	–[d]
	Tris.HCl buffer (pH 8.0)[]	604	–[d]	–[d]	96400	–[d]

[a] Stock solutions (1.0 mg/mL) of fluorophores/probes prepared in DMSO. [b] Only 0–0 band of the S_0-S_1 transition of hetero-rosamine unit is reported. [c] Determined using rhodamine 101 (Φ_F = 100% in MeOH, Ex at 530 nm for **3** and Ex at 550 nm for **1**, **2** and **4**) as a standard.[44] [d] No significant fluorescence emission that prevents determination of Stokes shift and relative fluorescence quantum yield. [VLKR = Valkyrie].

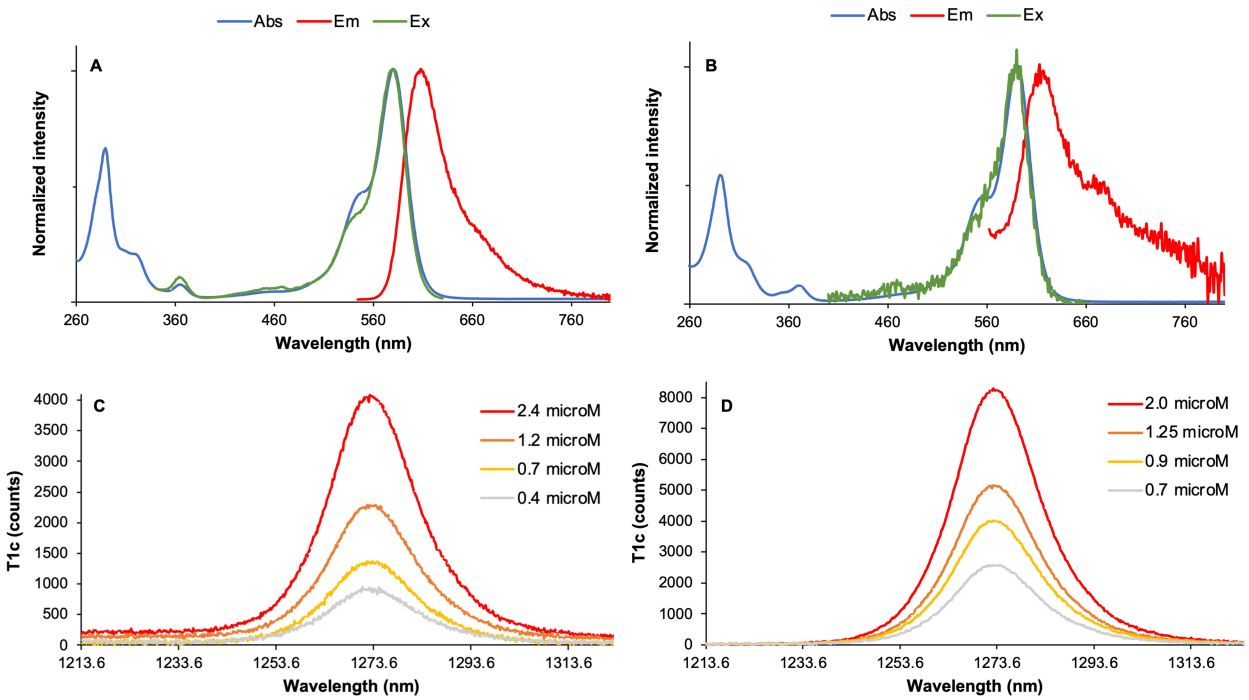

Figure 2. (top) Normalized UV-vis absorption, fluorescence emission and excitation spectra of hetero-rosamine dyes in PBS, at 25 °C: (A) S-rosamine **3**, (B) Se-rosamine **4**. (bottom) Singlet oxygen phosphorescence emission spectra of hetero-rosamine dyes in $CHCl_3$, at 20 °C, recorded with a liquid nitrogen-cooled InGaAs detector (CCD camera, multi-channel detector): (C) S-rosamine **3**, (D) Se-rosamine **4**. See Supporting Information for parameters used to record spectra.

characterized by a very modest quantum yield (1% in aq. buffers and 4% in DMSO respectively). Conversely, such residual far-red fluorescence was not readily detected in the case of selenium-containing Valkyrie probe **2**. As already observed for parent S-rosamine **3**, superimposition of absorption and excitation spectra was obtained for **1**, thus vividly illustrating

the positive contribution of phosphate and pyridinium moieties to make the ALP-responsive Valkyrie probes both water-soluble and not prone to self-aggregation in aqueous media.

Next, we studied the ability of S/Se-rosamine dyes **3** and **4** and related Valkyrie probes to produce $^1O_2$, aimed at revealing their claimed type-II (activatable) PS behavior.[3–4] Two distinct methods have been used to determine their singlet oxygen quantum yields (Φ_Δ). All obtained values are gathered in Table 2 to facilitate a comparative view. First, we took advantage of phosphorescence of $^1O_2$, centered at ca. 1270 nm,[31] to achieve relative determinations against a reference known to generate this ROS under excitation at the same wavelength. This is a fast and easy to implement method but the choice of measuring solvent is limited to chlorinated ($CHCl_3$ or CCl_4) or deuterated derivatives, to minimize non-radiative deactivation of $^1O_2$ strongly favored by X–H oscillators (X = N, O),[32] and thus increase its lifetime. We have chosen to work with $CHCl_3$ as solvent and zinc(II) tetraphenylporphyrin (ZnTPP) as reference ($\Phi_\Delta = 72\%$ in $CHCl_3$)[33] due to the good overlap of its first Q absorption band centered at ca. 550 nm, and the absorption profiles of our compounds. From a practical point of view, phosphorescence of $^1O_2$ was independently detected using two distinct instrumental setups: a CCD camera (multichannel detector) and a less sensitive single channel detector, both based on Indium-Gallium-Arsenic (InGaAs) semiconductor, cooled with liquid nitrogen. As expected, hetero-rosamine dyes **3** and **4** in solution in $CHCl_3$, showed strong phosphorescence at 1273–1275 nm upon excitation at 550 nm (Figure 2 and Figures S1-S2). Values of Φ_Δ are close to 30% and 60% respectively, again highlighting that the size of intracyclic chalcogen atom is of key importance in the modulation of ISC process which is operative for these hetero-xanthene-based molecules. Conversely, Valkyrie probes **1** and **2** exhibited very weak $^1O_2$ phosphorescence, only detectable with InGaAs/CCD camera (Figures S3–S4). Only with this intrumental setup, a singlet oxygen quantum yield of 3% was determined for **2**. All these results indicate that the ability of pyridine-hetero-rosamines to produce $^1O_2$, can be easily modulate through formal *N*-pyridyl alkylation-dealkylation process. We have also characterized the type-II photosensitizing properties of our compounds in less favourable protic solvents namely MeOH and EtOH (short lifetimes of $^1O_2$: 10 and 14 μs respectively, *vs.* 220 μs for $CHCl_3$).[34] To that end, a second comparative method based on UV-vis absorbance decay of $^1O_2$ chemical trap DPBF in the presence of each pyridine/pyridinium-hetero-rosamine or rose bengal (RB) selected as reference ($\Phi_\Delta = 76\%$ in MeOH, $\Phi_\Delta = 68\%$ in EtOH),[33] was used. Significant efforts have devoted to devise a robust and reliable protocol enabling accurate and repeatable measurements of relative singlet oxygen quantum yields. From a practical point of view, we have adapted a home-made irradiation device initially used for PDT experiments on cells conducted on a 96-well plate format. All control experiments done to ensure that results were consistent and repeatable, are summarized in the Supporting Information section. Thus, stability under green light irradiation ($\lambda_{max} = 530$ nm, wavelength range of 520–540 nm) of hetero-rosamine **3** and **4**, and related Valkyrie probes **1** and **2** was confirmed by UV-vis absorption spectroscopy, by subjecting them to 10 min illumination (*i.e.*, 10 times the delay required to achieve ROS generation) before recording the corresponding spectra. Furthermore, their respective dark stability (*i.e.*, in the absence of prior irradiation) was also assessed through periodic recording (every 5 min) of absorption at the corresponding wavelength maximum, within 30 min; for all compounds, the lack of spontaneous degradation or aggregation in MeOH (or in EtOH), was observed (Figures S7–S10 for illustrative examples of dark stability cuves). Thereafter, successive short-term irradiations (5 s) of alcoholic solutions containing compounds to be analyzed (or RB), in the presence of DPBF, led to a significant and gradual decrease of absorbance at 412 nm, thus indicating

Table 2. Singlet oxygen quantum yields (Φ_Δ [%]) hetero-rosamine dyes and ALP-responsive Valkyrie probes at 25 °C.

Cmpd[a]	Solvent	$^1O_2$ phosphorescence method (SCD)[b,c]	$^1O_2$ phosphorescence method (CCD)[c]	DPBF method[d]
3	$CHCl_3$	32	32	–[e]
	MeOH	n/a	n/a	11
	EtOH	n/a	n/a	10
4	$CHCl_3$	64	57	n/a
	MeOH	n/a	n/a	56
	EtOH	n/a	n/a	45
VLKR probe **1**	$CHCl_3$	–[e]	–[e]	n/a
	MeOH	n/a	n/a	–[e]
	EtOH	n/a	n/a	–[e]
VLKR probe **2**	$CHCl_3$	–[e]	3	n/a
	MeOH	n/a	n/a	–[e]
	EtOH	n/a	n/a	–[e]

[a] Stock solutions (1.0 mg/mL) of fluorophores/probes prepared in DMSO. [b] SCD = InGaAs single channel detector. [c] Determined using ZnTPP ($\Phi_\Delta = 72\%$ in $CHCl_3$, Ex at 550 nm) as a standard.[33] [d] Determined using RB ($\Phi_\Delta = 76\%$ in MeOH, $\Phi_\Delta = 68\%$ in EtOH, Ex at 550 nm) as a standard.[33] [e] No significant production of singlet oxygen that prevents determination of a relative quantum yield (assumed to be < 1%). [n/a = not applicable, VLKR = Valkyrie].

the conversion of $^1O_2$ chemical trap into *ortho*-dibenzoylbenzene through [4+2] cycloaddition with *in situ* generated singlet oxygen, and subsequent fragmentation of endoperoxide (Figure 3). The Φ_Δ values of hetero-rosamines **3** and **4** were calculated as 11% and 56% in MeOH, respectively; somewhat different values were obtained in EtOH: 10% and 45% respectively. For S-rosamine **3**, the significant difference between the found values of singlet oxygen quantum yield according to the method used (phosphorescence *vs.* DPBF), is explained by the change in the solvent ($CHCl_3$ *vs.* alcohols) that strongly impacts both fluorescence lifetime and quantum yield but also the propensity to undergo ISC to T_1 state. Given its spectral features respectively found in $CHCl_3$ ($\Phi_F = 31\%$ and fluorescence lifetime $\tau = 1.45$ ns, see Supporting Information for the corresponding spectra and decay curve) and MeOH ($\Phi_F = 16\%$ and fluorescence lifetime $\tau = 0.8$ ns, see Supporting Information for the corresponding spectra and decay curve), we hypothesized that protic solvents such as MeOH favors non-radiative relaxation pathways of the excited of S_1 state of **3**. In accordance with our starting hypothesis related to excited state quenching by d-PeT mechanism, and singlet oxygen phosphorescence measurements, pyridinium-based probes **1** and **2** were identified as poor type-II PS and it was not possible to determine the corresponding Φ_Δ values (less than 1%).

As conclusion of the comprehensive photophysical study, spectral features of hetero-rosamines and Valkyrie probes confirm that *N*-pyridyl alkylation-dealkylation process may be a feasible way to devise a novel PS activation strategy from hetero-xanthenes bearing this optically tunable group as *meso*-substituent. It is also interesting to emphasize the dual functionality of S-rosamine dye **3** as fluorophore and type-II photosensitizer. This makes this compound especially well-suited for the design of molecular phototheranostic platforms enabling early fluorescence diagnosis and therapy (PDT) concurrently under photo-irradiation.[35]

In vitro validations of ALP-responsive Valkyrie probes

As demonstrated in our contributions devoted to analytical validations of different classes of enzyme-responsive fluorogenic platforms,[30,36] it is of prime importance to combine conventional fluorescence-based assays with complementary RP-HPLC-fluorescence and RP-HPLC-MS analyses, to confirm the sensing mechanism of such probes. This is also the only way for assessing both efficacy and selectivity of the studied enzyme-triggered cascade reaction (conversion rate and possible formation of side-products). The good fluorescence properties of S-rosamine dye **3** in aqueous physiological conditions led us to examine the enzymatic activation of Valkyrie probe **1** through a conventional fluorescence-based assay involving time-course measurements (Figure 4). Upon addition of ALP (from calf intestine, 10 U) to a 1 μM solution of probe in PBS (pH 7.3) at 37 °C, a gradual increase in the orange-red fluorescence emission at 605 nm was observed, thus suggesting *in situ* release of intact pyridine-S-rosamine. An enzymatic incubation time of 205 min yielded a dramatic 79-fold increase in the signal intensity. Even if starting probe exhibits a weak ICT far-red emission, its fluorogenic behavior may be referred as the intensometric "OFF-ON" response mode. Typically, the use of Tris.HCl buffer (10 mM, pH 8.0) is preferred to PBS for such *in vitro* bioassays because ALP is known to have highest activity in this aq. medium. Conversely, this enzyme is known to be partly inhibited by mM concentrations of inorganic phosphate. When ALP-mediated activation of Valkyrie probe **1** was achieved in Tris.HCl buffer, a fastest kinetics was obtained: fluorescence intensity reached a plateau in less than 40 min, and a very high "OFF-ON" response up to 126-fold was obtained after 53 min of incubation (Figure S24). However, blank experiment conducted without enzyme has highlighted the moderate stability of Valkyrie probe **1** in Tris.HCl buffer, likely because the marked reactivity of its benzyl pyridinium moiety towards nucleophilic Tris (tris(hydroxymethyl)aminomethane) molecules leading to the premature removal of phosphatase recognition moiety (Figure S24). Such non-specific probe activation did not occur in PBS even if the partial inhibition of ALP by phosphate ions has considerably slowed down reaction kinetics. The ALP-triggered conversion of Valkyrie probe **1** into S-rosamine **3** was further supported by RP-HPLC analyses of crude enzymatic mixtures that combine both fluorescence and ESI-MS detection (see Figures S26–S43 for the RP-HPLC-fluorescence elution profiles and Figures S60-S64 for SIM analyses). As shown in

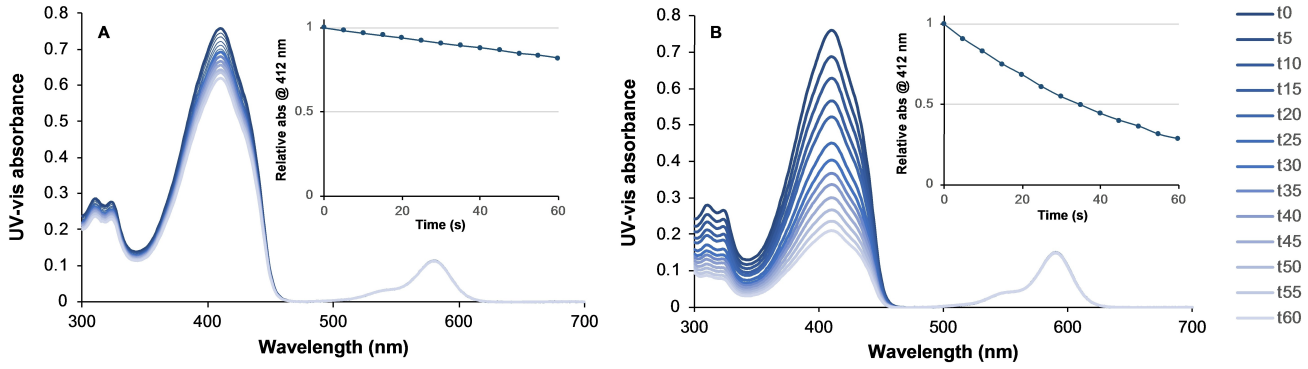

Figure 3. Absorption spectral change of DPBF in the presence of S-rosamine **3** (A) or Se-rosamine **4** (B) with green irradiation (λ_{max} 530 nm). All measurements were performed with a DPBF concentration of 37 μM in MeOH at 25 °C (concentration of hetero-rosamine dye: 1.15 μM for **3** and 1.25 μM for **4**). The data were acquired every 5 seconds. Inset: plot of absorption measured at 412 nm against time.

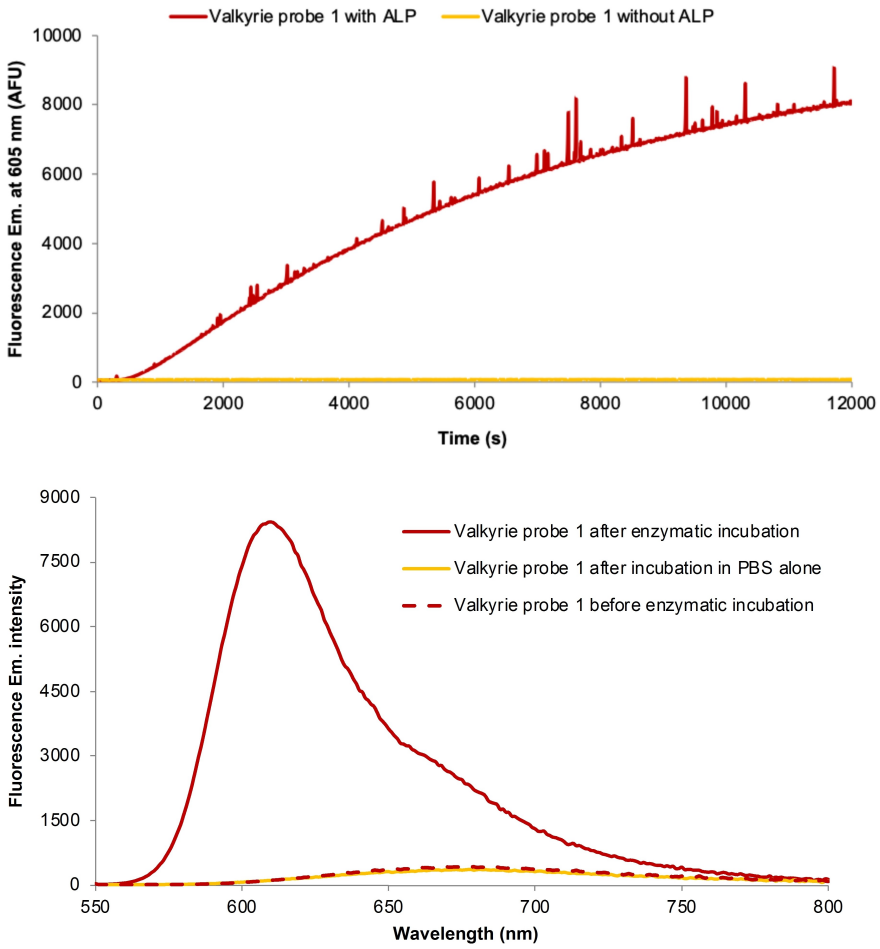

Figure 4. (A) Fluorescence emission time course (Ex/Em 540/605 nm, slits 5 nm) of sulfur-containing Valkyrie probe **1**, concentration: 1.0 μM, in the presence of ALP (10 U) in PBS (10 mM phosphate + 2.7 mM KCl and 137 mM NaCl, pH 7.3) at 37 °C. ALP was added after 5 min of incubation in PBS alone. (B) Overlay of fluorescence emission spectra (Ex at 540 nm, slits 5 nm) of sulfur-containing Valkyrie probe **1** before and after incubation with ALP. Please note: spike signals observed on the fluorescence kinetics curve are due to magnetic stirring.

Figure 5, the major peak at $t_R = 3.7$ min was unambiguously assigned to the released fluorophore (Abs $\lambda_{max} = 584$ nm, MS-(ESI+): $m/z = 360.3$ $[M]^+$, calcd for $C_{22}H_{22}N_3S^+$ 360.2). The two other very small peaks observed at $t_R = 3.2$ min and $t_R = 3.6$ min respectively, were identified as the starting Valkyrie probe **1** (Abs $\lambda_{max} = 598$ nm, MS(ESI+): $m/z = 360.2$ $[M^{2+} - C_7H_8O_4P^+]^+$ (fragmentation of benzyl pyridinium during the ionization process), calcd for $C_{29}H_{29}N_3O_4PS_2^+$ 546.2) and mono-*N*-demethylated product **9** ($\lambda_{max} = 570$ nm, MS(ESI+): $m/z = 346.3$ $[M]^+$, calcd for $C_{21}H_{20}N_3O_7^+$ 346.1). This latter unsymmetrical S-rosamine was formed through the oxidative photobluing pathway (*i.e.*, photooxidative dealkylation) frequently observed with fluorescent dyes bearing dialkylamino auxochromic groups subjected to continuous and/or high photonic excitation[37] (in our case, prolonged excitation involved in time-course fluorescence measurements). Gratifyingly, the "clean" appearance of collected elution chromatograms confirms that the fluorogenic cascade reaction triggered by ALP (*i.e.*, phosphate ester hydrolysis followed by *N*-dealkylation of quaternary pyrdinium moiety through 1,6-elimination) is univocal. Even if Se-rosamine dye **2** exhibits poor fluorescence properties, we managed to achieve *in vitro* validations of its ALP-responsive Valkyrie probe **4** according to the same analytical methodology described above for its sulfur counterpart (see Figures S25, S44-S59 and S65–S69). Almost quantitative conversion of such pyridinium-based probe into the parent photosensitizer upon enzymatic cleavage, was obtained. Finally, we explored the feasibility of devising an original luminescence assay for highlighting enzymatic activation of aPSs lacking (significant) fluorogenicity as is the case with compounds bearing heavy atoms such as iodine or selenium. We thus considered $^1O_2$ phosphorescence time-course measurements of Valkyrie probe **2** dissolved in a deuterated buffer (freeze-dried Tris.HCl buffer resuspended in D_2O, 10 mM, pH 8.2) and incubated with 10 U of ALP at 37 °C. At the time of these preliminary experiments, only InGaAs single channel detector (less sensitive than CCD camera) was available. Moreover, since $^1O_2$ lifetime in heavy water remains short (67 μs)[4b] and that this ROS may be also deactivated by non-deuterated Tris molecules containing three C–H oscillators, visualization of its phosphorescence signal was challenging and only possible by summing 10 successive spectra recorded in the range 1100–1400 nm (excitation at 590 nm, total duration of one cycle of acquisition: 460 s). This non-fluorogenic phosphatase assay consisted of performing 25

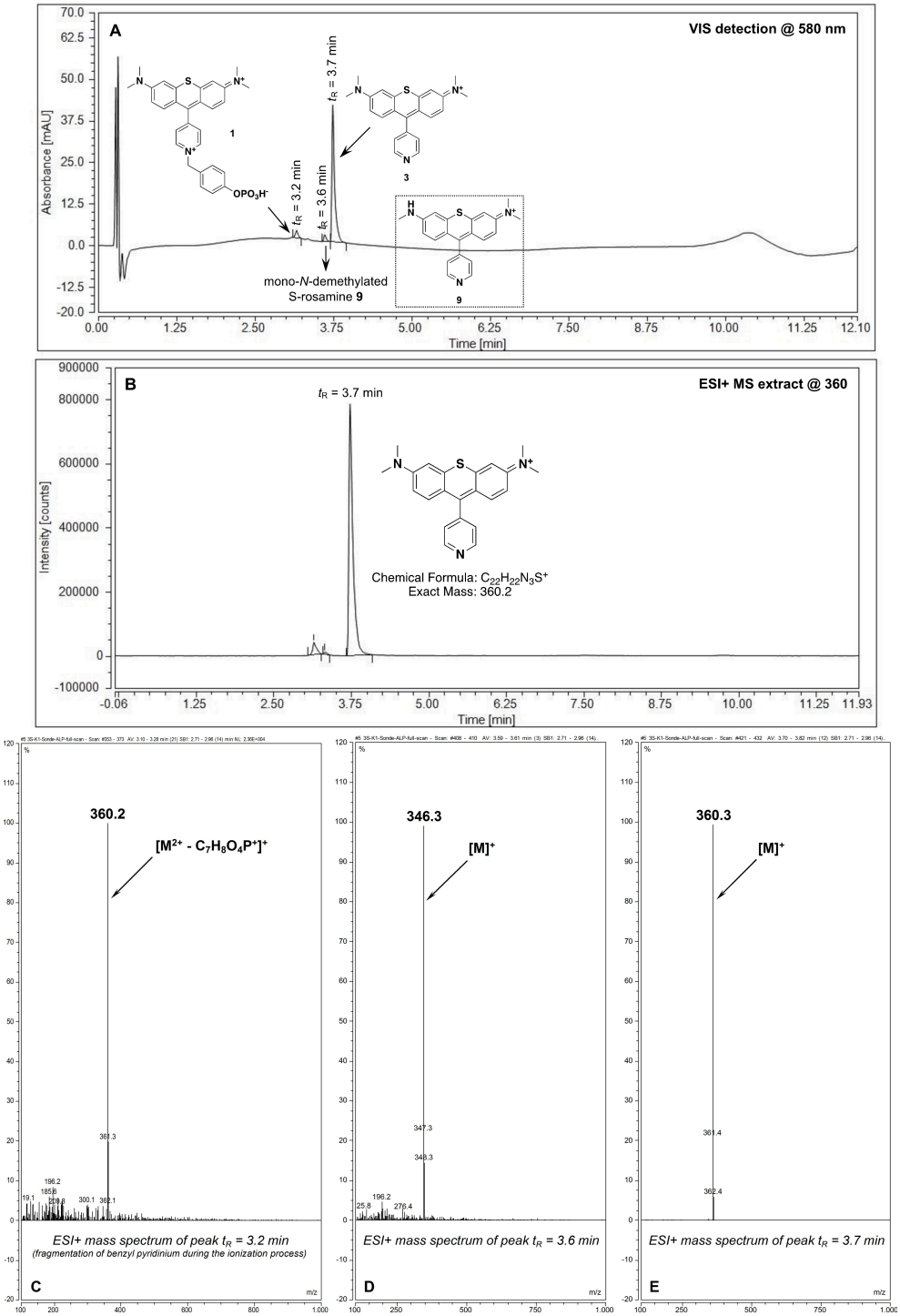

Figure 5. RP-HPLC elution profiles of enzymatic reaction mixture of Valkyrie probe **1** with ALP (after 205 min of incubation). (A) Visible detection at 580 nm; dotted frame: structure of mono-*N*-demethylated S-rosamine **9**. (B) ESI + TIC channel (MS extract at 360 a.m.u.). (C) ESI + mass spectrum of peak at $t_R = 3.2$ min. (D) ESI + mass spectrum of peak at $t_R = 3.6$ min. (E) ESI + mass spectrum of peak at $t_R = 3.7$ min. [a] See Supporting Information for details about chromatographic system used (system S1).

cycles (ca. 3 h). As displayed in Figure 6A, addition of ALP led to an increase of $^1O_2$ phosphorescence centered at ca. 1275 nm thereby confirming both the release of Se-rosamine PS **4** and its ability to produce $^1O_2$ in this enzymatic reaction mixture. However, after having reached a maximum intensity within 23 min, the phosphorescence curve gradually decreased thus indicating of a slow degradation of **4** through photooxidation and/or photo-assisted reaction with solvent molecules (*i.e.*, Tris molecules) At the end of this 3 h enzyme assay, direct UV-vis absorption analysis of the reaction mixture revealed partial loss of visible absorption signature of this hetero-xanthene, as compared with the intensity obtained with a solution of Se-

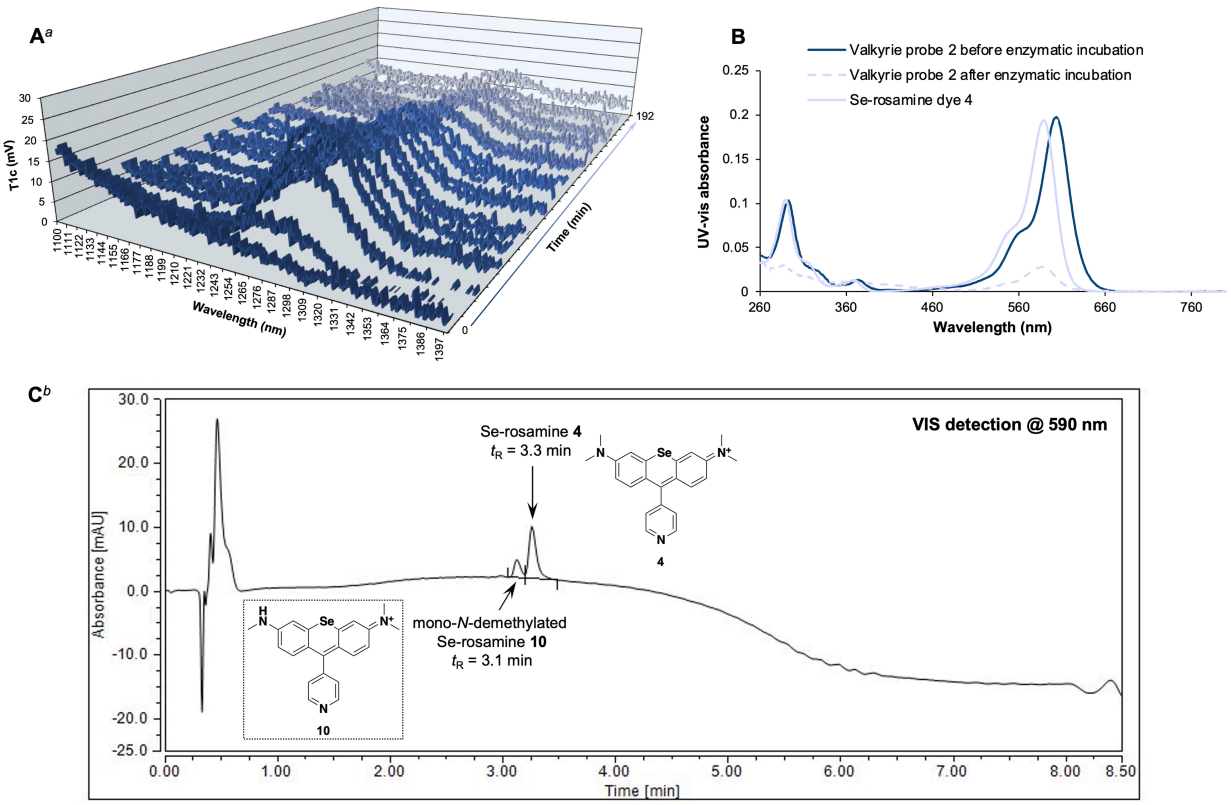

Figure 6. Non-fluorogenic phosphatase assay with selenium-containing Valkyrie probe **2** (incubation time: 192 min). (A) 3D plot time course measurement of singlet oxygen phosphorescence emission spectra of Valkyrie probe **2**, concentration: 2.5 μM, in the presence of ALP (10 U) in Tris.HCl buffer (prepared in D_2O, 10 mM, pH 8.2) at 37 °C. ALP was added after the first cycle of aquisition. (B) Overlay UV-vis absorption spectra of Valkyrie probe **2** before and after this phosphatase assay, and Se-rosamine **4** (2.5 μM solution prepared in Tris.HCl/D_2O buffer), recorded at 25 °C. (C) RP-HPLC elution profile of enzymatic reaction mixture after 192 min of incubation, visible detection at 590 nm; dotted frame: structure of mono-*N*-demethylated Se-rosamine **10**. [a] Singlet oxygen phosphorescence emission spectra were recorded with liquid nitrogen-cooled InGaAs single channel detector, see Experimental Section for parameters used to record spectra. [b] See Supporting Information for details about chromatographic system used (system S2), and UV-vis absorption and ESI + mass spectra of peaks at t_R = 3.1 min and 3.3 min (Figures S70–71).

rosamine **4** prepared at the same concentration (Figure 6B), thus supporting the moderate stability of this PS under prolonged photoexcitation at 590 nm. Further investigations will be done to precisely characterize this degradation pathway. However, RP-HPLC-MS analyses (Figure 6C and Figures S70–71) confirmed the enzyme-mediated release of this hetero-rosamine **2** from the corresponding Valkyrie probe **2** (t_R = 3.3 min, Abs λ_{max} = 594 nm, MS(ESI+): *m/z* = 408.3 $[M]^+$, calcd for $C_{22}H_{22}N_3Se^+$ 408.1) and its partial conversion into mono-*N*-demethylated derivative **10** (t_R = 3.1 min, Abs λ_{max} = 582 nm, MS(ESI+): *m/z* = 394.1 $[M]^+$, calcd for $C_{21}H_{20}N_3Se^+$ 394.1). Major improvements will also be brought to this original assay format to perform facile/rapid validation of aPSs in a more accurate and reliable manner.

All the collected data allowed us to confirm the viability and effectiveness of the photosensitizer activation strategy applied to *meso*-pyridyl-substituted S-/Se-pyronins and based on pyridine caging/decaging chemistry.

Conclusions

In summary, we devised a short and efficient synthetic route to S- and Se-rosamines bearing 4-pyridyl moiety as *meso* aryl substituent. The availability of these unusual hetero-xanthene dyes and their facile derivatization through formal pyridine quaternarization, enabled us to access to Valkyrie probes. This novel class of innovative organic photosensitizers has been rationally designed to be responsive to a specific disease biomarker (typically, an enzyme) and thus suitable for targeted PDT. The proposed activation strategy is based on the effective modulation of d-PeT process between hetero-pyronin unit and *meso*-pyridyl group through a change in the *N*-substitution/charge state of the pyridine substituent (*i.e.*, cationic pyridinium *vs.* neutral pyridine). This yields an "OFF-ON" response mode for both type-II photosensitizing (singlet oxygen generation) and orange-red fluorescence properties. This caging/decaging strategy was successfully implemented with the preparation of "proof-of-concept" ALP-responsive Valkyrie probes **1** and **2** containing 4-phosphoryloxybenzyl moiety as *N*-alkyl substituent of *meso*-pyridinium. Their selective activation by ALP, thereby restoring fluorescence emission and/or singlet oxygen generation was demonstrated by means of *in vitro* studies involving a

combination of fluorescence- and $^1O_2$ phosphorescence enzyme assays, complemented by RP-HPLC analyses (UV-vis, fluorescence and ESI-MS detection). This robust analytical methodology also provided a set of data that confirmed the proposed enzyme-triggered cascade reaction. Since the Valkyrie probe design principle combines two well-established and proven concepts, we are convinced of its practical utility, whether to design smarter therapeutic agents suitable for first-line treatment of cancer/infection, or for the rapid construction of multifunctional small-molecule (photo)theranostic agents using fluorescence as diagnostic modality.[14a,c,38] Indeed, the heteroatom-substitution approach is intensively used to readily convert conventional O-xanthene dyes into superior fluorophores and/or photosensitizers.[39] The flexibility of pyridine caging/decaging strategy proposed by the Ge group,[21] is obvious because its implementation to a wide range of different reactive biomarkers will only require a minor structural alteration, namely the replacement of recognition moiety introduced onto the self-immolative benzyl-pyridinium linker.[40]

Experimental Section

General

Unless otherwise noted, all commercially available reagents and solvents were used without further purification. TLC was carried out on Merck Millipore DC Kieselgel 60 F-254 aluminum sheets (Merck). The spots were directly visualized or through illumination with a UV lamp ($\lambda = 254/365$ nm). All purifications by flash-column chromatography were performed on "small" granulometry silica gel (40–63 μm) from VWR. HPLC-grade DCM and MeCN were dried over alumina cartridges immediately prior to use (water content: 50 ppm for DCM and 75 ppm for MeCN, determined by Karl Fischer titration[41]), using a solvent purification system PureSolv PS-MD-5 model from Innovative Technology. DMF was purchased from Fisher Chemical (>99%, lab reagent grade), dried by storage over activated 3 Å molecular sieves and kept under Ar atmosphere. HPLC-gradient grade acetonitrile (MeCN) was obtained from Fisher Chemical. All aqueous buffers used in this work and aqueous mobile-phases for RP-HPLC were prepared using water purified with a PURELAB Ultra system (ELGA, VEOLIA, purified to 18.2 MΩ cm). 4-(Bromomethyl)phenyl diethyl phosphate **8** [916661-26-2], 3-iodo-*N*,*N*-dimethylaniline [33454-16-9] and 3,3′-thiobis[*N*,*N*-dimethylbenzeneamine] **5** [935467-69-9] were prepared according to literature procedures.[26–28]

Instruments and Methods

Freeze-drying operations were performed with a Christ Alpha 2–4 LD plus. Centrifugation steps were performed with a Sprout® Plus Mini Centrifuge instrument (Heathrow Scientific). ^{1}H-, ^{13}C-, ^{19}F-, ^{31}P- and ^{77}Se-NMR spectra were recorded either on a Bruker Avance Neo 500 MHz (equipped with a 5 mm BBOF iProbe) or on a Bruker Avance III HD 600 MHz spectrometer (equipped with a 5 mm BBOF CryoProbe Prodigy). NMR spectroscopy chemical shifts are quoted in parts per million (δ) relative to TMS (for ^{1}H, and ^{13}C), $CFCl_3$ (for ^{19}F), aq. 85% H_3PO_4 (for ^{31}P) or Me_2Se (for ^{77}Se). For ^{1}H and ^{13}C spectra, calibration was made by using residual signals of partially deuterated solvent summarized in 2010 by Fulmer *et al.*[42] For all other nuclei, SR value obtained after zero-calibration of the corresponding reference was applied. *J* values are expressed in Hz. IR spectra were recorded with a Bruker Alpha FT-IR spectrometer equipped with a universal ATR sampling accessory. The bond vibration frequencies are expressed in reciprocal centimeters (cm^{-1}). RP-HPLC-MS analyses were performed on a Thermo-Dionex Ultimate 3000 instrument (pump + autosampler at 20 °C + column oven at 25 °C) equipped with a diode array detector (Thermo-Dionex DAD 3000-RS) and MSQ Plus single quadrupole mass spectrometer. Purifications by semi-preparative HPLC were performed on a Thermo-Dionex Ultimate 3000 instrument (semi-preparative pump HPG-3200BX) equipped with an RS Variable Detector (VWD-3400RS, four distinct wavelengths within the range 190–800 nm). Ion chromatography analyses (for the determination of TFA mass content in freeze-dried samples) were performed using a Thermo Scientific Dionex ICS 6000 ion chromatograph equipped with a conductivity detector CD (Thermo Scientific Dionex) and a conductivity suppressor ADRS 600 2 mm (Thermo Scientific Dionex), and according to a method developed by the PACSMUB staff.[43] Low-resolution mass spectra (LRMS) were recorded on a Thermo Scientific MSQ Plus single quadrupole instrument equipped with an electrospray (ESI) source. See Supporting Information for all details related to instruments and methods for photophysical characterizations of hetero-rosamine dyes and Valkyrie probes.

High-Performance Liquid Chromatography Separations

Several chromatographic systems were used for the analytical experiments and the purification steps: System A: RP-HPLC-MS (Phenomenex Kinetex C_{18} column, 2.6 μm, 2.1×50 mm) with MeCN (+0.1% FA) and 0.1% aq. formic acid (aq. FA, pH 2.1) as eluents [5% MeCN (0.1 min) followed by a linear gradient from 5% to 100% (5 min) of MeCN, then 100% MeCN (1.5 min)] at a flow rate of 0.5 mL/min. UV-visible detection was achieved at 220, 260, 290 and 590 nm (+DAD 220–800 nm allowing extraction of any single wavelength channel within this spectral range). Low resolution ESI-MS detection (MSQ Plus) in the positive/negative mode (full scan, 100–1000 a.m.u., spectrum type: centroid, needle voltage: 3.0 kV, probe temperature: 350 °C, cone voltage: 75 V and scan time: 1 s). System B: semi-preparative RP-HPLC (SiliCycle SiliaChrom C_{18} column, 10 μm, 20×250 mm) with MeCN and aq. 0.1% TFA (pH 1.9) as eluents [10% MeCN (5 min), followed by a gradient from 10% to 20% MeCN (7.5 min), then 20% to 100% MeCN (93 min)] at a flow rate of 20.0 mL/min. Quadruple UV-visible detection was achieved at 220, 260, 285 and 585 nm. System C: system B with the following gradient [5% MeCN (5 min), followed by a gradient from 5% to 10% MeCN (7.5 min), then 10% to 100% MeCN (105 min)]. Quadruple UV-visible detection was achieved at 220, 260, 290 and 590 nm. System D: system B with quadruple UV-visible detection at 220, 260, 290 and 595 nm. System E: system C with quadruple UV-visible detection at 220, 260, 290 and 605 nm. System F: system A with the following gradient [5% MeCN (0.1 min) followed by a linear gradient from 5% to 100% (5 min) of MeCN, then 100% MeCN (3 min)] and fluorescence detection (at 45 °C) with the following sets of parameters: (1) S-rosamine **3** and Valkyrie probe **1**, Ex/Em channels 580/610 nm and 595/680 nm (sensitivity: 1, PMT: Auto, filter wheel: Auto); (2) Se-rosamine **4** and Valkyrie probe **2**, Ex/Em channels 590/615 nm and 605/680 nm (sensitivity: 1, PMT: Auto, filter wheel: Auto).

Syntheses

Please note: sodium selenide (Na_2Se) is a highly hazardous substance (acute toxic if inhaled or swallowed, prolonged or repeated exposure may cause organ injury, very toxic for (aquatic) environment). For handling this chemical, please work under a well-ventilated fume hood, wear protective gloves (two pairs) and goggles. Please oxidize

all residual/trace amounts of Na_2Se derivatives (assumed to be present in aq. phases after extraction, on the outer surface of the gloves, …) by overnight incubation with bleach, H_2O_2 and EtOH. The resulting solution will be next transferred into a special tank devoted to the storage of heavy metal wastes. Thereafter, this tank will be collected and treated by a specialist firm.

S-Rosamine dye 3

Symmetrical bis-aryl sulfide [935467-69-9] **5** (100 mg, 0.37 mmol, 1 equiv.) and 4-pyridinecarboxaldehyde (47 mg, 0.44 mmol, 1.2 equiv.) were mixed in a sealed tube and dissolved in propionic acid (3 mL). A catalytic amount of *p*-TSA (6.3 mg, 0.037 mmol, 0.1 equiv.) was added and the resulting reaction mixture was heated at 120 °C for 3 h. The reaction was checked for completion by RP-HPLC-MS (system A). Thereafter, the mixture was diluted with an aq. 5% solution of K_2CO_3 and extracted thrice with DCM. Combined organic phases were dried over anhydrous $MgSO_4$, filtered and concentrated under reduced pressure. The resulting crude product was purified by semi-preparative RP-HPLC (system B, t_R = 20–27 min). The product containing fractions were lyophilized to give TFA salt of S-rosamine **3** as a dark purple amorphous powder (41 mg, 0.06 mmol, yield 16% based on TFA mass = 48.17% determined by ion chromatography). IR (ATR): ν = 3089, 2515, 2171, 1777, 1664, 1594, 1499, 1449, 1397, 1368, 1347, 1262, 1179, 1128, 1060, 998, 956, 917, 834, 812, 794, 722; ^{1}H NMR (500 MHz, [D$_6$]DMSO): δ = 8.92 (d, *J* = 5.3 Hz, 2H), 7.69–7.55 (m, 2H), 7.47 (d, *J* = 2.3 Hz, 2H), 7.18 (d, *J* = 9.7 Hz, 2H), 7.15 (dd, *J* = 9.7, *J* = 2.5 Hz, 2H), 3.26 (s, 12H); ^{13}C NMR (126 MHz, [D$_6$]DMSO): δ = 164.4, 162.8, 158.8, 154.2, 152.6, 144.7, 134.0, 126.6, 125.6, 115.7, 49.9; ^{19}F NMR (470 MHz, [D$_6$]DMSO): δ = −74.6 (s, 3F, C*F*$_3$-TFA); HPLC (system A): t_R = 3.6 min (purity > 99% at 290 nm and > 99% at 590 nm); LRMS (ESI+, recorded during RP-HPLC analysis): *m/z* 360.4 $[M]^+$ (100), calcd for $C_{22}H_{22}N_3S^+$ 360.2; UV-vis (recorded during RP-HPLC analysis): λ_{max} = 244, 289 and 584 nm; UV-vis (DMSO, 25 °C): λ_{max} = 292 nm (ε 56 200 M^{-1} cm^{-1}) and 591 nm (ε 98 050 M^{-1} cm^{-1}); UV-vis (PBS, pH 7.3, 25 °C): λ_{max} = 289 nm (ε 56 400 M^{-1} cm^{-1}) and 581 nm (ε 86 750 M^{-1} cm^{-1}); UV-vis (Tris.HCl buffer, pH 8.0, 25 °C): λ_{max} = 289 nm (ε 56 800 M^{-1} cm^{-1}) and 580 nm (ε 89 950 M^{-1} cm^{-1}); Fluorescence ($CHCl_3$, 25 °C): λ_{max} = 597 nm, Φ_F = 31%, τ (nanoLED @ 592 nm) = 1.45 ns; Fluorescence (DMSO, 25 °C): λ_{max} = 621 nm, Φ_F = 19%, τ (nanoLED @ 592 nm) = 1.1 ns; Fluorescence (MeOH, 25 °C): λ_{max} = 605 nm, Φ_F = 16%, τ (nanoLED @ 592 nm) = 0.8 ns; Fluorescence (PBS, pH 7.3, 25 °C): λ_{max} = 608 nm, Φ_F = 14%, τ (nanoLED @ 592 nm) = 0.9 ns; Fluorescence (Tris.HCl buffer, pH 8.0, 25 °C): λ_{max} = 605 nm, Φ_F = 14%, τ (nanoLED @ 592 nm) = 0.8 ns.

Symmetrical bis-aryl selenoether 6

*Please note: this compound is already registered by Chemical Abstracts, CAS number [935467-70-2], and referenced in only one publication (Holt et al.),[29] source: SciFinder^n. However, this article does not described the synthesis and use of 3,3′-selenobis[N,N-dimethylbenzenamine] but those of the corresponding diseleno derivative **7**, registered with a different CAS number [85670-00-4]. We identified this indexing error during the course of our work.*

3-Iodo-*N*,*N*-dimethylaniline [33454-16-9] (247 mg, 1 mmol, 1.7 equiv.) and Na_2Se (75 mg, 0.6 mmol, 1 equiv.) were placed in a sealed tube, solubilized in dry DMF (2 mL) and kept under Ar atmosphere. Then, CuI (19 mg, 0.1 mmol, 0.17 equiv.) and anhydrous K_2CO_3 (138 mg, 1 mmol, 1.7 equiv.) were sequentially added and the resulting reaction mixture was stirred at 120 °C overnight. After 12 h of heating, a further amount of Na_2Se (75 mg, 0.6 mmol, 1 equiv.) was added and the mixture was stirred at 120 °C for one additional night. The reaction was checked for completion by RP-HPLC-MS (system A) and diluted with EtOAc. Then, the resulting mixture was washed thrice with deionized H_2O, dried over anhydrous $MgSO_4$, filtered and concentrated under reduced pressure. The resulting residue was purified by flash-column chromatography over silica gel (bed size: 30×120 mm eluent: step gradient of DCM in heptane from 50% to 100%) to give 3,3′-selenobis[*N*,*N*-dimethylbenzenamine] **6** as a colorless oil (31 mg, 0.1 mmol, yield 31%). IR (ATR): ν = 3411, 3072, 2877, 2802, 1911, 1725, 1581, 1554, 1489, 1439, 1395, 1314, 1289, 1228, 1179, 1123, 1095, 1095, 1060, 981, 953, 829, 758; ^{1}H NMR (500 MHz, $CDCl_3$): δ = 7.21–7.10 (m, 2H), 6.92 (s, 2H), 6.87–6.80 (m, 2H), 6.71–6.61 (m, 2H), 2.92 (s, 12 H); ^{13}C NMR (126 MHz, $CDCl_3$): δ = 151.0, 132.0, 129.8, 121.3, 117.0, 111.7, 40.7; ^{77}Se NMR (95 MHz, $CDCl_3$): δ = 426.2 (s, 1Se); HPLC (system A): t_R = 4.3 min (purity 91% at 260 nm); LRMS (ESI+, recorded during RP-HPLC analysis): *m/z* 321.3 $[M+H]^+$ (100) and 362.3 $[M+H+MeCN]^+$ (80), calcd for $C_{16}H_{21}N_2Se^+$ 321.1; UV (recorded during RP-HPLC analysis): λ_{max} = 260 nm.

Se-Rosamine dye 4

3,3′-Selenobis[*N*,*N*-dimethylbenzenamine] **6** (30 mg, 0.094 mmol, 1 equiv.) and 4-pyridinecarboxaldehyde (20 mg, 0.19 mmol, 2 equiv.) were mixed in a sealed tube and dissolved in propionic acid (1 mL). A catalytic amount of *p*-TSA (1.6 mg, 0.0094 mmol, 0.1 equiv.) was added and the resulting reaction mixture was heated at 120 °C for 3 h, and then cooled to RT. Thereafter, *p*-chloranil (23 mg, 0.094 mmol, 1 equiv.) was added and the mixture was stirred at RT for further 2 h. The reaction was checked for completion by RP-HPLC-MS (system A). Thereafter, the mixture was directed diluted with aq. 0.1% TFA (without prior evaporation of propionic acid) and purified by semi-preparative RP-HPLC (system D, t_R = 22–28 min). The product containing fractions were lyophilized to give TFA salt of Se-rosamine **4** as a dark blue amorphous powder (16 mg, 0.023 mmol, yield 24% based on TFA mass = 42.87% determined by ion chromatography). IR (ATR): ν = 2362, 2186, 2171, 2148, 2105, 2078, 2035, 1992, 1957, 1667, 1600, 1500, 1451, 1400, 1373, 1349, 1267, 1196, 1167, 1135, 1002, 953, 918, 853, 835, 798, 779, 722, 708; ^{1}H NMR (500 MHz, [D$_6$]DMSO): δ = 8.90 (d, *J* = 4.9 Hz, 2H), 7.76 (dd, *J* = 2.7, *J* = 1.3 Hz, 2H), 7.63–7.54 (m, 2H), 7.17 (d, *J* = 9.7 Hz, 2H), 7.11–7.00 (m, 2H), 3.23 (s, 12H); ^{13}C NMR (151 MHz, [D$_6$]DMSO): δ = 165.7, 162.3, 158.7, 155.7, 154.1, 146.5, 134.0, 127.2, 125.1, 119.3, 49.8; ^{19}F NMR (565 MHz, [D$_6$]DMSO): δ = −74.5 (s, 3F, C*F*$_3$-TFA); ^{77}Se NMR (115 MHz, [D6]DMSO): δ = 478.2 (s, 1Se); HPLC (system A): t_R = 3.6 min (purity 99% at 290 nm and 99% at 590 nm); LRMS (ESI+, recorded during RP-HPLC analysis): *m/z* 408.3 $[M]^+$ (100), calcd for $C_{22}H_{22}N_3Se^+$ 408.1; UV-vis (recorded during RP-HPLC analysis): λ_{max} = 245, 291 and 595 nm; UV-vis (DMSO, 25 °C): λ_{max} = 294 nm (ε 56 350 M^{-1} cm^{-1}) and 601 nm (ε 114 000 M^{-1} cm^{-1}); UV-vis (PBS, pH 7.3, 25 °C): λ_{max} = 291 nm (ε 53 820 M^{-1} cm^{-1}) and 591 nm (ε 101 600 M^{-1} cm^{-1}); UV-vis (Tris.HCl buffer, pH 8.0, 25 °C): λ_{max} = 291 nm (ε 57 300 M^{-1} cm^{-1}) and 590 nm (ε 112 500 M^{-1} cm^{-1}).

Sulfur-containing Valkyrie probe 1

S-Rosamine **3** (20 mg, 55 μmol, 1 equiv.) and 4-(bromomethyl)phenyl diethyl phosphate [916661-26-2] **8** (35 mg, 110 μmol, 2 equiv.) were mixed and dissolved in dry MeCN (2 mL). The resulting reaction mixture was refluxed overnight. The reaction was checked for completion by RP-HPLC-MS (system A) and the mixture was concentrated under reduced pressure. The resulting residue was dissolved in dry DCM (2 mL) and kept under under Ar atmosphere. Then, TMSBr (37 μL, 280 μmol, 5 equiv.) was added and the reaction mixture was stirred at RT for 22 h. The progress of phosphate deprotection was checked for completion by RP-HPLC-

MS (system A) and the mixture was quenched by addition of MeOH (2 mL). After evaporation under reduced pressure, the crude product was diluted with aq. 0.1% TFA and purified by semi-preparative RP-HPLC (system C, t_R = 29.5–32 min). The product containing fractions were lyophilized to give TFA salt of Valkyrie probe **1** as a dark blue amorphous powder (9.3 mg, 12 μmol, yield 22% based on TFA mass = 28.93% determined by ion chromatography). IR (ATR): ν = 3403, 3051, 2930, 1685, 1638, 1592, 1501, 1449, 1397, 1366, 1344, 1256, 1162, 1124, 958, 918, 795, 743, 715; ^{1}H NMR (500 MHz, [D$_6$]DMSO): δ = 9.45 (d, *J* = 6.2 Hz, 2H), 8.35 (d, *J* = 6.1 Hz, 2H), 7.71 (d, *J* = 8.2 Hz, 2H), 7.53 (d, *J* = 2.5 Hz, 2H), 7.30 (d, *J* = 8.2 Hz, 2H), 7.23 (d, *J* = 9.7 Hz, 2H), 7.09 (dd, *J* = 9.7, *J* = 2.6 Hz, 2H), 5.93 (s, 1H), 3.29 (s, 12H); ^{13}C NMR (151 MHz, [D$_6$]DMSO): δ = 162.8, 162.2, 161.1, 154.9, 152.4, 144.7, 140.4, 138.7, 138.3, 130.1, 130.1, 126.2, 125.6, 116.0, 72.4, 50.0; ^{19}F NMR (565 MHz, [D$_6$]DMSO): δ = −73.5 (s, 3F, C*F*$_3$-TFA); ^{31}P NMR (243 MHz, [D$_6$]DMSO): δ = −6.3 (s, 1P, *P*-phosphate); HPLC (system A): t_R = 3.1 min (purity 97% at 290 nm and 97% at 590 nm); LRMS (ESI+, recorded during RP-HPLC analysis): *m/z* 360.4 [M^{2+} - $C_7H_8O_4P^+$]$^+$ (100) *fragmentation of benzyl pyridinium during the ionization process*, and 546.2 [M^{2+} - H]$^+$ (2), calcd for $C_{29}H_{29}N_3O_4PS^+$ 546.2; UV-vis (recorded during RP-HPLC analysis): λ_{max} = 245, 291 and 596 nm; UV-vis (DMSO, 25 °C): λ_{max} = 294 nm (ε 48 500 M^{-1} cm^{-1}) and 602 nm (ε 77 050 M^{-1} cm^{-1}); UV-vis (PBS, pH 7.3, 25 °C): λ_{max} = 291 nm (ε 53 250 M^{-1} cm^{-1}) and 595 nm (ε 81 750 M^{-1} cm^{-1}); UV-vis (Tris.HCl buffer, pH 8.0, 25 °C): λ_{max} = 291 nm (ε 52 200 M^{-1} cm^{-1}) and 594 nm (ε 78 850 M^{-1} cm^{-1}); Fluorescence (DMSO, 25 °C): λ_{max} = 677 nm, Φ_F = 4%; Fluorescence (PBS, pH 7.3, 25 °C): λ_{max} = 678 nm, Φ_F = 1%; Fluorescence (Tris.HCl buffer, pH 8.0, 25 °C): λ_{max} = 678 nm, Φ_F = 1%.

Selenium-containing Valkyrie probe 2

Se-Rosamine **4** (14 mg, 34 μmol, 1 equiv.) and 4-(bromomethyl)phenyl diethyl phosphate [916661-26-2] **8** (22 mg, 68 μmol, 2 equiv.) were mixed and dissolved in dry MeCN (1.1 mL). The resulting reaction mixture was refluxed overnight. The reaction was checked for completion by RP-HPLC-MS (system A) and the mixture was concentrated under reduced pressure. The resulting residue was dissolved in dry DCM (1.25 mL) and kept under Ar atmosphere. Then, TMSBr (23 μL, 17 μmol, 5 equiv.) was added and the reaction mixture was stirred at RT for 22 h. The progress of phosphate deprotection was checked for completion by RP-HPLC-MS (system A) and the mixture was quenched by addition of MeOH (2 mL). After evaporation under reduced pressure, the crude product was diluted with aq. 0.1% TFA and purified by semi-preparative RP-HPLC (system E, t_R = 29.5–32.5 min). The product containing fractions were lyophilized to give TFA salt of Valkyrie probe **2** as a dark blue amorphous powder (9.5 mg, 11 μmol, yield 32% based on TFA mass = 32.83% determined by ion chromatography). IR (ATR): ν = 2929, 2204, 2102, 2034, 1986, 1685, 1595, 1498, 1450, 1396, 1369, 1346, 1260, 1167, 1127, 954, 918, 835, 814, 796, 782, 739, 715; ^{1}H NMR (500 MHz, [D$_6$]DMSO): δ = 9.43 (d, *J* = 6.3 Hz, 2H), 8.38–8.24 (m, 2H), 7.82 (d, *J* = 2.7 Hz, 2H), 7.71 (d, *J* = 8.6 Hz, 2H), 7.30 (d, *J* = 8.2 Hz, 2H), 7.21 (d, *J* = 9.7 Hz, 2H), 6.99 (dd, *J* = 9.7, *J* = 2.6 Hz, 2H), 5.92 (s, 1H), 3.26 (s, 12H); ^{13}C NMR (151 MHz, [D$_6$]DMSO) δ = 154.7, 153.4, 153.3, 145.8, 144.9, 137.5, 131.5, 129.6, 129.4, 128.0, 121.1, 121.1, 117.8, 116.2, 110.6, 40.9; ^{19}F NMR (565 MHz, [D$_6$]DMSO): δ = −74.0 (s, 3F, C*F*$_3$-TFA); ^{31}P NMR (243 MHz, [D$_6$]DMSO): δ = −6.4 (s, 1P, *P*-phosphate); ^{77}Se NMR (115 MHz, [D$_6$]DMSO): δ = 481.5; HPLC (system A): t_R = 3.1 min (purity 98.5% at 290 nm and 98% at 590 nm); LRMS (ESI+, recorded during RP-HPLC analysis): *m/z* 408.5 [M^{2+} - $C_7H_8O_4P^+$]$^+$ (100) *fragmentation of benzyl pyridinium during the ionization process*, and 595.4 [M^{2+} - H]$^+$ (3), calcd for $C_{29}H_{29}N_3O_4PSe^+$ 594.1; UV-vis (recorded during RP-HPLC analysis): λ_{max} = 248, 293 and 605 nm; UV-vis (DMSO, 25 °C): λ_{max} = 296 nm (ε 44 200 M^{-1} cm^{-1}) and 611 nm (ε 79 500 M^{-1} cm^{-1}); UV-vis (PBS, pH 7.3, 25 °C): λ_{max} = 293 nm (ε 49 150 M^{-1} cm^{-1}) and 604 nm (ε 96 300 M^{-1} cm^{-1}); UV-vis (Tris.HCl buffer, pH 8.0, 25 °C): λ_{max} = 293 nm (ε 50 700 M^{-1} cm^{-1}) and 604 nm (ε 96 400 M^{-1} cm^{-1}).

In vitro Activation of ALP-Responsive Valkyrie Probes

Experimental details about stock solutions of fluorophores, probes, enzyme and buffers

- All 1.0 mg/mL stock solutions of fluorophores (**3** and **4**) and ALP-responsive Valkyrie probes (**1** and **2**) were prepared in DMSO (UV-spectroscopy grade, Honeywell Riedel-de-Haën). *Please note: these solutions were stored at 4 °C (frozen DMSO) and found to be full-stable even after 2 years.*
- Commercial ALP (from calf intestine, #P4978, 10 U/μL, storage buffer: 10 mM Tris.HCl (pH 8.2), 50 mM KCl, 1 mM $MgCl_2$, 0.1 mM $ZnCl_2$, 50% glycerol, Sigma-Aldrich) was stored at −20 °C and directly used without dilution.
- Phosphate-buffered saline (PBS, 10 mM phosphate + 2.7 mM KCl and 137 mM NaCl, pH 7.3). This buffer was prepared by dissolving one PBS tablet (#BP2944-100, Fisher BioReagents™) in 200 mL of ultrapure H_2O.
- Tris.HCl buffer (10 mM, pH 8.0) prepared either in ultrapure H_2O or freeze-dried and dissolved in D_2O (99.9% D, #D214F, Eurisotop).

Fluorescence-based bioassays

All assays were performed at 37 °C (using a Lauda Ecoline Recirculating Chiller RE 106 combined with a temperature controller Lauda E100, connected to the spectrofluorometer cell holder) and conducted with magnetic stirring. Probe's concentration in 3.5 mL fluorescence quartz cell was set to 1.0 μM. Whatever the buffer used (PBS or Tris.HCl buffer), the volume of the probe's solution was always 3.0 mL. Depending on the Valkyrie probe studied, the following sets of detection parameters were used:

- Sulfur-containing Valkyrie probe **1**, Ex/Em 540/605, slits 5 nm,
- Selenium-containing Valkyrie probe **2**, Ex/Em 550/615, slits 5 nm.

Fluorescence emission of the released hetero-rosamine was monitored at the suitable Ex/Em wavelength pair, over time with measurements every 5 s (duration of assay: 200 min). 10 U (1.0 μL) of ALP was added after 5 min of incubation in buffer alone. Blank experiments to assess the stability of the Valkyrie probes in buffers, were achieved in the same way but without adding ALP. For each kinetics, fluorescence emission spectrum of Valkyrie probe was recorded before and after enzymatic activation or incubation in buffer alone, with the following sets of parameters:

- Sulfur-containing Valkyrie probe **1**, Ex 540 nm (slit 5 nm), Em 550–800 nm (slit 5 nm),
- Selenium-containing Valkyrie probe **2**, Ex 550 nm (slit 5 nm), Em 560–800 nm (slit 5 nm).

Singlet oxygen phosphorescence-based bioassay

This assay was performed at 37 °C (using a Lauda Ecoline Recirculating Chiller RE 106 combined with a temperature controller Lauda E100, connected to the spectrofluorometer cell holder) and conducted with magnetic stirring. Selenium-containing Valkyrie probe's concentration in 3.5 mL fluorescence quartz cell was set to 2.5 μM. Tris.HCl buffer prepared in D_2O was used (10 mM, pH 8.2), the volume of the probe's solution was 3.0 mL. $^1O_2$ phosphorescence generated by the released Se-rosamine **4** was monitored

through the recording of SWIR emission spectra in the range 1100–1400 nm (excitation at 590 nm, total duration of one cycle of acquisition corresponding to the sum of 10 successive spectra: 460 s). This non-fluorogenic phosphatase assay consisted of performing 25 cycles (ca. 3 h).

RP-HPLC-fluorescence and RP-HPLC-MS (full scan and SIM modes) analyses

Enzymatic reaction mixtures from fluorescence-based *in vitro* assays were directly analyzed by RP-HPLC-fluorescence (injected volume: 20 μL, system F). In some cases, samples have been frozen with liquid nitrogen and stored at −25 °C. Defrosting and subsequent RP-HPLC analyses were considered only when instrument was available.

Thereafter, each enzymatic reaction mixture (3 mL) was freeze-dried; the resulting white amorphous powder was dissolved in a 2:1 (v/v) mixture of ultrapure H_2O and MeCN (total volume = 600 μL). The solution was vortexed followed by centrifugation (6000 rpm, 30 s). 20 μL of supernatant was injected into the HPLC-MS apparatus (system S1, see Supporting Information).

Please note: injection of buffer (PBS or Tris.HCl buffer) was also achieved immediately prior to each SIM analysis, especially to confirm the lack of residual contaminants within the C_{18} column or ESI probe at the corresponding m/z value selected for the SIM detection mode and then avoid misinterpretations.

Acknowledgements

This work is part of the project "MULTIMOD", supported by the Conseil Régional de Bourgogne Franche-Comté and the European Union through the PO FEDER-FSE Bourgogne 2014/2020 programs. Financial supports from Agence Nationale de la Recherche (ANR, AAPG 2018, PRCI, LuminoManufacOligo, ANR-18-CE07-0045; AAPG 2021, PRC, InnoTherano, ANR-21-CE07-0010), especially for the post-doc fellowship of Dr. Kévin Renault and for the purchase of InGaAs single channel detector are also greatly acknowledged. GDR CNRS "Agents d'Imagerie Moléculaire" (AIM) 2037 is also thanked for its interest in this work related to the research topic "small-molecule phototheranostics". The authors (affiliated to ICMUB lab) thank the "Plateforme d'Analyse Chimique et de Synthèse Moléculaire de l'Université de Bourgogne" (PACSMUB, http://www.wpcm.fr) for access to analytical and molecular spectroscopy instruments. The authors (affiliated to ICMUB lab) also thank Dr. Richard A Decréau (University of Burgundy, ICMUB, thesis supervisor of VL) for his relevant scientific suggestions and the loan of home-made irradiation device used in this work, Dr. Myriam Laly (University of Burgundy, PACSMUB) for the determination of TFA content in fluorophore/probe samples, Drs. Quentin Bonnin (CNRS, PACSMUB) and Michel Picquet (University of Burgundy, ICMUB, PACSMUB) for their assistance during the recording of ^{77}Se NMR spectra, Mr. Cédric Balan (University of Burgundy, ICMUB, PACSMUB) for Karl Fischer titrations, Mr. Emilien Sezeur (2nd year IUT student, IUT Le Mans, 2019–2020) for the synthesis of symmetrical bis-aryl thioether (3,3′-thiobis[*N*,*N*-dimethylbenzeneamine) **5**, Drs. Philippe Arnoux (Laboratoire Réactions et Génie des Procédés, UMR 7274, Nancy) and Yann Bretonnière (Laboratoire de Chimie de l'ENS Lyon, UMR 5182) for their good advices in singlet oxygen phosphorescence measurements, and Dr. Yoan Capello (UBFC, ICMUB) for a critical reading of manuscript before submission.

Conflict of Interests

The authors declare no conflict of interest.

Data Availability Statement

The data that support the findings of this study are available from the corresponding author upon reasonable request.

[1] For selected reviews about targeted approaches in therapy, see: a) M. G. Sikkandhar, A. M. Nedumaran, R. Ravichandar, S. Singh, I. Santhakumar, Z. C. Goh, S. Mishra, G. Archunan, B. Gulyás, P. Padmanabhan, *Int. J. Mol. Sci.* **2017**, *18*, 1036; b) S. S. Bashraheel, A. Domling, S. K. Goda, *Biomed. Pharmacother.* **2020**, *125*, 110009.
[2] a) T. J. Dougherty, *Crit. Rev. Oncol. Hematol.* **1984**, *2*, 83–116; b) P. Agostinis, K. Berg, K. A. Cengel, T. H. Foster, A. W. Girotti, S. O. Gollnick, S. M. Hahn, M. R. Hamblin, A. Juzeniene, D. Kessel, M. Korbelik, J. Moan, P. Mroz, D. Nowis, J. Piette, B. C. Wilson, J. Golab, *Ca-Cancer J. Clin.* **2011**, *61*, 250–281.
[3] M. S. Baptista, J. Cadet, P. Di Mascio, A. A. Ghogare, A. Greer, M. R. Hamblin, C. Lorente, S. C. Nunez, M. S. Ribeiro, A. H. Thomas, M. Vignoni, T. M. Yoshimura, *Photochem. Photobiol.* **2017**, *93*, 912–919.
[4] a) A. Greer, *Acc. Chem. Res.* **2006**, *39*, 797–804; b) P. R. Ogilby, *Chem. Soc. Rev.* **2010**, *39*, 3181–3209.
[5] a) M. S. Baptista, J. Cadet, A. Greer, A. H. Thomas, *Photochem. Photobiol.* **2021**, *97*, 1456–1483; b) J. Fujii, Y. Soma, Y. Matsuda, *Molecules* **2023**, *28*, 4085.
[6] a) T. C. Pham, V.-N. Nguyen, Y. Choi, S. Lee, J. Yoon, *Chem. Rev.* **2021**, *121*, 13454–13619; b) N. Mariño-Ocampo, L. Dibona-Villanueva, E. Escobar-Álvarez, D. Guerra-Díaz, D. Zúñiga-Núñez, D. Fuentealba, J. Robinson-Duggon, *Photochem. Photobiol.* **2023**, *99*, 469–497; c) L. K. B. Tam, D. K. P. Ng, *Mater. Chem. Front.* **2023**, *7*, 3184–3193.
[7] For selected reviews about photosensitizer-antibody conjugates in photo-immunotherapy, see: a) P. M. R. Pereira, B. Korsak, B. Sarmento, R. J. Schneider, R. Fernandes, J. P. C. Tomé, *Org. Biomol. Chem.* **2015**, *13*, 2518–2529; b) S. R. G. Fernandes, R. Fernandes, B. Sarmento, P. M. R. Pereira, J. P. C. Tomé, *Org. Biomol. Chem.* **2019**, *17*, 2579–2593; c) J. Sandland, R. W. Boyle, *Bioconjugate Chem.* **2019**, *30*, 975–993.
[8] R. Hudson, M. Carcenac, K. Smith, L. Madden, O. J. Clarke, A. Pèlegrin, J. Greenman, R. W. Boyle, *Br. J. Cancer* **2005**, *92*, 1442–1449.
[9] Y. Tang, D. Lee, J. Wang, G. Li, J. Yu, W. Lin, J. Yoon, *Chem. Soc. Rev.* **2015**, *44*, 5003–5015.
[10] S. Singha, Y. W. Jun, S. Sarkar, K. H. Ahn, *Acc. Chem. Res.* **2019**, *52*, 2571–2581.
[11] For reviews about activatable photosensitizers, see: a) J. F. Lovell, T. W. B. Liu, J. Chen, G. Zheng, *Chem. Rev.* **2010**, *110*, 2839–2857; b) P. Majumdar, R. Nomula, J. Zhao, *J. Mater. Chem. C* **2014**, *2*, 5982–5997; c) X. Li, S. Kolemen, J. Yoon, E. U. Akkaya, *Adv. Funct. Mater.* **2017**, *27*, 1604053; d) M. Liu, C. Li, *ChemPlusChem* **2020**, *85*, 948–957; e) X. Zhao, J. Liu, J. Fan, H. Chao, X. Peng, *Chem. Soc. Rev.* **2021**, *50*, 4185–4219; f) Z. Li, Z. Zhou, Y. Wang, J. Wang, L. Zhou, H.-B. Cheng, J. Yoon, *Coord. Chem. Rev.* **2023**, *493*, 215324.
[12] A. M. Bugaj, *Photochem. Photobiol. Sci.* **2011**, *10*, 1097–1109.
[13] For a review about activatable photosensitizers based on a bioorthogonal trigger, see: E. Kozma, M. Bojtár, P. Kele, *Angew. Chem. Int. Ed.* **2023**, *62*, e202303198.
[14] For selected reviews, see: a) P. Cheng, K. Pu, *ACS Appl. Mater. Interfaces* **2020**, *12*, 5286–5299; b) P. Sarbadhikary, B. P. George, H. Abrahamse, *Theranostics* **2021**, *11*, 9054–9088; c) X. Yin, Y. Cheng, Y. Feng, W. R. Stiles, S. H. Park, H. Kang, H. S. Choi, *Adv. Drug Deliv.* **2022**, *189*, 114483.
[15] a) M. R. Detty, P. N. Prasad, D. J. Donnelly, T. Ohulchanskyy, S. L. Gibson, R. Hilf, *Bioorg. Med. Chem.* **2004**, *12*, 2537–2544; b) T. Y. Ohulchanskyy,

D. J. Donnelly, M. R. Detty, P. N. Prasad, *J. Phys. Chem. B* **2004**, *108*, 8668–8672.
[16] R. P. Sabatini, M. F. Mark, D. J. Mark, M. W. Kryman, J. E. Hill, W. W. Brennessel, M. R. Detty, R. Eisenberg, D. W. McCamant, *Photochem. Photobiol. Sci.* **2016**, *15*, 1417–1432.
[17] a) J. E. Hill, M. K. Linder, K. S. Davies, G. A. Sawada, J. Morgan, T. Y. Ohulchanskyy, M. R. Detty, *J. Med. Chem.* **2014**, *57*, 8622–8634; b) K. S. Davies, M. K. Linder, M. W. Kryman, M. R. Detty, *Bioorg. Med. Chem.* **2016**, *24*, 3908–3917.
[18] A. Mukaimine, T. Hirayama, H. Nagasawa, *Org. Biomol. Chem.* **2021**, *19*, 3611–3619.
[19] a) Y. Ichikawa, M. Kamiya, F. Obata, M. Miura, T. Terai, T. Komatsu, T. Ueno, K. Hanaoka, T. Nagano, Y. Urano, *Angew. Chem. Int. Ed.* **2014**, *53*, 6772–6775; b) M. Chiba, Y. Ichikawa, M. Kamiya, T. Komatsu, T. Ueno, K. Hanaoka, T. Nagano, N. Lange, Y. Urano, *Angew. Chem. Int. Ed.* **2017**, *56*, 10418–10422; c) W. Piao, K. Hanaoka, T. Fujisawa, S. Takeuchi, T. Komatsu, T. Ueno, T. Terai, T. Tahara, T. Nagano, Y. Urano, *J. Am. Chem. Soc.* **2017**, *139*, 13713–13719; d) M. Chiba, M. Kamiya, K. Tsuda-Sakurai, Y. Fujisawa, H. Kosakamoto, R. Kojima, M. Miura, Y. Urano, *ACS Cent. Sci.* **2019**, *5*, 1676–1681.
[20] For examples of "smart" Se-rhodamine/rosamine-based photosensitizers activated by non-enzymatic stimuli (*i.e.*, reducing agents), see: a) W. Lv, S. Chi, W. Feng, T. Liang, D. Song, Z. Liu, *Chem. Commun.* **2019**, *55*, 7037–7040; b) F. Ponte, G. Mazzone, N. Russo, E. Sicilia, *Chem. Eur. J.* **2022**, *28*, e202104083.
[21] a) Y. Wang, L. Yang, X.-R. Wei, R. Sun, Y.-J. Xu, J.-F. Ge, *Anal. Methods* **2018**, *10*, 5291–5296; b) L. Yang, J.-Y. Niu, R. Sun, Y.-J. Xu, J.-F. Ge, *Analyst* **2018**, *143*, 1813–1819; c) L. Yang, J.-Y. Niu, R. Sun, Y.-J. Xu, J.-F. Ge, *Sens. Actuators B* **2018**, *259*, 299–306.
[22] A. Leite, L. Cunha-Silva, D. Silva, A. I. M. C. Lobo Ferreira, L. M. N. B. F. Santos, I. C. S. Cardoso, V. L. M. Silva, M. Rangel, A. M. G. Silva, *Chem. Eur. J.* **2019**, *25*, 15073–15082.
[23] a) H. Zhang, K. Li, L.-L. Li, K.-K. Yu, X.-Y. Liu, M.-Y. Li, N. Wang, Y.-H. Liu, X.-Q. Yu, *Chin. Chem. Lett.* **2019**, *30*, 1063–1066; b) Z. Zhou, X. Yuan, D. Long, M. Liu, K. Li, Y. Xie, *Spectrochim. Acta Part A* **2021**, *246*, 118927.
[24] For examples of "smart" type II photosensitizers activated by ALP, see: a) W. Zhai, Y. Zhang, M. Liu, H. Zhang, J. Zhang, C. Li, *Angew. Chem. Int. Ed.* **2019**, *58*, 16601–16609; b) J. Fang, Y. Feng, Y. Zhang, A. Wang, J. Li, C. Cui, Y. Guo, J. Zhu, Z. Lv, Z. Zhao, C. Xu, H. Shi, *J. Am. Chem. Soc.* **2022**, *144*, 23061–23072.
[25] K. Wang, W. Wang, X.-Y. Zhang, A.-Q. Jiang, Y.-S. Yang, H.-L. Zhu, *TrAC Trends Anal. Chem.* **2021**, *136*, 116189.
[26] J. Park, Y. Kim, *Bioorg. Med. Chem. Lett.* **2013**, *23*, 2332–2335.
[27] P. M. Liu, C. G. Frost, *Org. Lett.* **2013**, *15*, 5862–5865.
[28] F. Deng, L. Liu, W. Huang, C. Huang, Q. Qiao, Z. Xu, *Spectrochim. Acta Part A* **2020**, *240*, 118466.
[29] J. J. Holt, B. D. Calitree, J. Vincek, M. K. Gannon, M. R. Detty, *J. Org. Chem.* **2007**, *72*, 2690–2693.
[30] K. Renault, Y. Capello, S. Yao, S. Halila, A. Romieu, *Chem. Asian J.* **2023**, *18*, e202300258.
[31] A. A. Krasnovsky Jr, *Photochem. Photobiol.* **1979**, *29*, 29–36.
[32] R. Schmidt, H. D. Brauer, *J. Am. Chem. Soc.* **1987**, *109*, 6976–6981.
[33] R. W. Redmond, J. N. Gamlin, *Photochem. Photobiol.* **1999**, *70*, 391–475.
[34] M. Elsherbini, R. K. Allemann, T. Wirth, *Chem. Eur. J.* **2019**, *25*, 12486–12490.
[35] For selected examples of S-containing organic dyes acting as both fluorophore and photosensitizer, see: a) S. Yao, Y. Chen, W. Ding, F. Xu, Z. Liu, Y. Li, Y. Wu, S. Li, W. He, Z. Guo, *Chem. Sci.* **2023**, *14*, 1234–1243; b) B. Wang, Y. Huang, D. Yang, J. Xu, X. Zhong, S. Zhao, H. Liang, *J. Mater. Chem. B* **2023**.
[36] S. Jenni, F. Ponsot, P. Baroux, L. Collard, T. Ikeno, K. Hanaoka, V. Quesneau, K. Renault, A. Romieu, *Spectrochim. Acta Part A* **2021**, *248*, 119179.
[37] A. N. Butkevich, M. L. Bossi, G. Lukinavičius, S. W. Hell, *J. Am. Chem. Soc.* **2019**, *141*, 981–989.
[38] H.-H. Han, H.-M. Wang, P. Jangili, M. Li, L. Wu, Y. Zang, A. C. Sedgwick, J. Li, X.-P. He, T. D. James, J. S. Kim, *Chem. Soc. Rev.* **2023**, *52*, 879–920.
[39] a) F. Deng, Z. Xu, *Chin. Chem. Lett.* **2019**, *30*, 1667–1681; b) L. Wang, W. Du, Z. Hu, K. Uvdal, L. Li, W. Huang, *Angew. Chem., Int. Ed.* **2019**, *58*, 14026–14043.
[40] For a recent extension of pyridine caging/decaging chemistry to tyrosinase enzyme, see: I. Verirsen, B. Uyar, N. G. Ozsamur, N. Demirok, S. Erbas-Cakmak, *Org. Biomol. Chem.* **2022**, *20*, 8864–8868.
[41] A. S. Meyer, C. M. Boyd, *Anal. Chem.* **1959**, *31*, 215–219.
[42] G. R. Fulmer, A. J. M. Miller, N. H. Sherden, H. E. Gottlieb, A. Nudelman, B. M. Stoltz, J. E. Bercaw, K. I. Goldberg, *Organometallics* **2010**, *29*, 2176–2179.
[43] G. Dejouy, M. Laly, I. E. Valverde, A. Romieu, *Dyes Pigm.* **2018**, *159*, 262–274.
[44] A. M. Brouwer, *Pure Appl. Chem.* **2011**, *83*, 2213–2228.

Manuscript received: August 29, 2023
Revised manuscript received: October 6, 2023
Accepted manuscript online: October 9, 2023
Version of record online: October 20, 2023

Correction added on 2.11.2023: Correction in graphical abstract.